Bursting Events in the Stable Atmospheric Boundary Layer

by

JULIE ANN PHILLIPSON, B.S.

A THESIS

in

ATMOSPHERIC SCIENCE

Submitted to the Graduate Faculty
of Texas Tech University in
Partial Fulfillment of
the Requirements for
the Degree of
MASTER OF SCIENCE

Approved by:

Dr. Sukanta Basu
Committee Chairman

Dr. Xiaoning Gilliam
Committee Co-Chair

Dr. Colleen Leary
Associate Chair

Dr. Fred Hartmeister
Dean of the Graduate School

May, 2008

ACKNOWLEDGMENTS

I would first like to thank Sukanta Basu for all of his help, patience, and encouragement he has given to me over the past two years. His guidance and his expertise on the topic, which was completely new to me, helped to keep me from feeling overwhelmed when I easily could have been. I would also like to thank Xiaoning Gilliam for her guidance and unique mathematical approach to my topic, which I would not have considered without her assistance. Also, Colleen Leary, I acknowledge for her continued interest in my project, and helpful suggestions that served to open my eyes to new possibilities not only concerning my research, but concerning my path through and after academia. Finally, I am grateful to Suraj Harshan for the patience and help he offered to me and for providing me with the WRF model output that was very important to this project.

My parents have always been a source of unconditional love and support for me, and have continued to do so more than ever since I have been at Texas Tech University. Their words of encouragement and faith in me have helped immensely, and I would not have made it this far without them. My close friends here in Lubbock and abroad have also helped me, likely more than they know, always there to offer support when I've needed it most. It is because of these people, my family and my friends, that I've come as far as I have, and been blessed with my success. For all of them, I'll be forever grateful.

This work was partially funded by the Texas Advanced Research Program (003644-0003-2006) and the National Science Foundation (ANT-0538453) grants.

TABLE OF CONTENTS

ABSTRACT

Though recent experiments and field projects regarding the characteristics of the boundary layer have been conducted, there is still an overall lack of understanding about the mechanics of the stable boundary layer, whether it is transitionally stable, such as the nocturnal stable boundary layer in mid-latitudes, or persistently stable, such as the boundary layer in Polar Regions. ISCAT-00 is one such field project conducted in Antarctica, where an instrumented tower was used to record wind speed and temperature information, from which heat and momentum flux transfers can be discerned. Understanding of boundary layer processes is especially important for the stable layer since despite its stable nature, sporadic bursts of turbulence have been observed to occur, indicated by data collected from the ISCAT-00 campaign. These bursts, though short-lived, are responsible for most of the heat and momentum transfer that occurs within the otherwise stable layer. Since these bursts of turbulence disrupt the stable layer, they can not only pose problems for air quality forecasts, but they can also inhibit the performance of wind turbines. Transient loading from these bursting events as rotor blades pass through patches of organized, coherent turbulence can shorten the life span of a wind turbine by 5 to 10 years. However, despite the noted occurrence of turbulence bursting in the stable layer there is still very little known about its origins, causes, or basic properties.

In order to explore the characteristics of turbulent bursting events in the stable layer, two methodologies are applied to analyze data obtained from the

ISCAT00 campaign. The first methodology applied to discern the occurrence of turbulent bursting is one created by Nakamura & Mahrt (2005). The second methodology is a newly developed adaptive threshold methodology, which is much more robust, and removes much of the subjectivity of other turbulence bursting identification methods. The adaptive technique allows for the reduction of subjectivity in the data analysis phase, and is therefore felt to be more accurate. Also, spectral characteristics of polar turbulence are explored, and are found to have similar properties to spectra observed in mid-latitudes. This research focuses primarily on different methods, both old and newly developed that can help to further understanding about turbulence in the stable boundary layer and the corresponding heat and moisture flux properties.

LIST OF FIGURES

LIST OF TABLES

CHAPTER 1

INTRODUCTION AND BACKGROUND INFORMATION

1.1 Introduction and Motivation

Over the course of a day, the atmospheric boundary layer (ABL) transitions between being neutral, convective, and stable in mid-latitudes. The convective, or mixed, layer tends to occur during peak heating during the daytime, when heat and momentum transfers are at maximum values. Much of this heat and momentum transfer occurs due to turbulent eddies that exist in the boundary layer, and can be increased due to large scale influences such as frontal passages, high wind events, or gravity wave phenomena. At sunset, outgoing longwave radiation from the surface begins to dominate the energy transfer in the boundary layer, and the mixed layer begins to gradually erode, being replaced by the developing stable boundary layer (SBL). As the night persists, the stable boundary layer continues to grow, eventually reaching depths of tens of meters to a couple hundred meters. However, the mixed layer from the daytime does not completely dissipate. Instead, it is displaced upward in the ABL, and is often referred to as the residual layer. In the residual layer, mixing continues to occur, though the stable layer below can be considered to essentially be decoupled from that above (Stull, 1988). Though the stable boundary layer is governed by primarily light winds, turbulence has been found to occur in the form of intermittent “bursts” (Mahrt, 1988; Narasimha and Kailas,

1989; Nappo, 1990; Chimonas, 1998; Sun et al., 2002; Van De Weil et al., 2002; Banta et al., 2003; Nakamura and Mahrt, 2005; and others), and these bursts have yet to be defined due to an overall lack of understanding as to their causes and properties.

The stable layer over the past decade has become more of a focus for study, as indicated by the Cooperative Atmosphere-Surface Exchange Study - 1999 (CASES-99) that was conducted in Kansas. Throughout the duration of the experiment, turbulent bursting events were found to have occurred in the nocturnal stable boundary layer, as highlighted by Sun et al. (2002), Van De Weil et al. (2003), and Nakamura and Mahrt (2005). More recently, a similar experiment was conducted on the Antarctic plateau, the Investigation of Sulfur Chemistry in the Antarctic Troposphere – 2000 (ISCAT00). Both of these experiments were conducted over flat, relatively homogeneous terrain; however CASES-99 focused on the mid-latitude, transitionally stable nocturnal boundary layer, whereas ISCAT-00 focused on the persistently stable boundary layer most often encountered in high latitudes. The primary difference between these two layers is that the residual layer found in mid-latitudes is not present at high latitudes. This is due to the fact that less solar radiation is received in Polar regions, and of radiation that does make it to the surface, nearly 72 percent is reflected due to high surface albedo (Hanson, 1961). Given the lack of surface heating, a convective or mixed layer never occurs, and stability persists not only during the night, but during the daytime as well. Though the ISCAT-00 study was

conducted with a focus on atmospheric chemistry, sporadic turbulent episodes were also found to have occurred, which could possibly have been due to katabatic wind events, or density currents (Davis et al., 2004; Oncley et al., 2004).

Both CASES-99 and ISCAT-00 were groundbreaking in that they provided an insight as to the properties of the stable layer and turbulence, which play a significant role in not only modeling the stable boundary layer, but also meteorological forecasting, air pollution dispersion forecasting, and wind energy applications. Current boundary layer models suffer when it comes to depicting the stable layer due to a lack of high-resolution in-situ measurements of SBL properties, and also because data collected at the surface are not representative of the stable layer as a whole (Salmond and McKendry, 2005). This directly impacts air quality forecasting, because pollutants are trapped close to the surface under the stable layer inversion. If turbulence is found to occur, pollutants can disperse, thereby nullifying a “bad air quality” forecast. Furthermore, when considering implications to wind energy, stable boundary layer turbulence can result in fatigue damage to wind turbines, effectively reducing their life span from nearly 20 years to 15 years, and sometimes even 10 (Kelley et al., 2005). This occurs due to transient loading on turbine rotor blades as they pass through areas of organized turbulence caused by vertical shear and strong temperature gradients.

Despite all previous studies, there is still no clear definition as to what a turbulent burst is, or what atmospheric conditions cause them to occur. Nakamura and Mahrt (2005) developed a methodology to detect these events, and building upon this existing coherent structure detection methodology, this research focuses on the development of a robust adaptive methodology to identify a turbulent event. Using tower data from the ISCAT-00 experiment and applying a new methodology, the goal is to have a more robust way of identifying the events, resulting in a better idea of how to forecast such events, allowing for improved modeling and meteorological understanding.

1.2 Causes of intermittent bursting

Though turbulent bursting in the stable layer has yet to be clearly defined, yet there are several possible causes outlined in existing literature. First, the Blackadar effect is considered. As stable stratification forms near the surface, heat and momentum fluxes are minimized, and due to lack of friction along the surface, turbulence is suppressed. This layer then, in turn, serves as a frictionless “surface” for the residual layer above, since fluxes are minimal across the boundary between these two layers. Flow then continues in the residual layer, due to larger scale influences such as mesoscale systems, resulting in larger shear values as the flow moves over the frictionless surface below. Once this shear is strong enough, the boundary of the stable layer can then be disrupted, allowing the faster moving flow to diffuse downward, resulting in a

turbulent burst. Another possible cause of bursting is the passage of a density current. Density current, in this case, can refer to a gravity wave, frontal passage, or outflow from a previously existing storm system. The propagation of the density current, characterized by lower pressure than the surrounding area and a higher velocity than the ambient environment is considered to be enough to disrupt the stable layer, resulting in turbulent eddies along its leading edge. One other cause, encountered with fair regularity in mid-latitudes, is the low-level jet. The low-level jet is primarily a nocturnal phenomenon, occurring in conjunction with increased radiative cooling at the surface and the subsequent decoupling of the stable layer from the residual layer above. The low-level jet tends to occur at the top of the stable layer, characterized by high velocity flow, and the nose of the jet can at times disrupt the top of the stable layer, resulting in a burst of turbulence. It is these turbulent events that are responsible for most of the vertical energy transfer in the stable layer.

1.3 Previous Studies of Atmospheric Bursting Events

Narasimha and Kailas (1989) describe two of the first studies of atmospheric turbulence events using tower data – the Monsoon Experiment (Bangalore) and another experiment conducted at the Boulder Atmospheric Observatory. In order to quantify the occurrence of bursting events, horizontal and vertical velocities were examined and flux values calculated, leading to further examination of ‘flux events’ that exhibit increased values compared to the

background data. After selecting and analyzing data sets from the Boulder tower during what was deemed to be neutrally stable stratification, Narasimha and Kailas (1989) found u'w' flux perturbation values exceeding the mean by upwards of 100 percent. Upon comparing these findings to those in Bangalore, similar characteristics were found using the Variable Interval Time Averaging (VITA) technique as developed by Blackwelder and Kaplan (1976). This technique allows for more in-depth analysis of intermittency imbedded within a signal by considering the short-term variance *D* of a turbulent quantity *p'* (Narasimha and Kailas, 1989)

$$D(p';t,t_{av}) \equiv \frac{1}{t_{av}} \int_{t-\frac{t_{av}}{2}}^{t+\frac{t_{av}}{2}} p'^{2}(s)ds - \left(\frac{1}{t_{av}} \int_{t-\frac{t_{av}}{2}}^{t+\frac{t_{av}}{2}} p'^{2}(s)ds\right)^{2} \tag{1.3.1}$$

where t_{av} is the time interval chosen. Furthermore, Narasimha and Kailas (1989) dictate that the mean square value of *p'* (1.3.2) is independent of the time step *t* in cases of stationary turbulence.

$$p^2 = \lim_{t_{av}\to\infty} D(p';t,t_{av}) \tag{1.3.2}$$

Using this technique and comparison between flux values, Narasimha and Kailas (1989) conclude that any time *D* surpasses a selected threshold, that the turbulent event would be indicated, being considered as an event of significant. They do note, however, that the suggested threshold and the interval of time averaging are both extremely subjective, as will be noted in other future methodologies as well.

After analysis, Narasimha and Kailas (1989) found that w' events were of much greater magnitude of u' events, and occur at shorter time scales. Furthermore, they found through comparison of analyzed data that using their VITA technique, identified turbulent bursting events accounted for much more of the flux transport than did the mean flow, supporting the theoretical basis for stable boundary layer processes.

In his 1988 study, Mahrt presented the idea that it was "necessary to distinguish between small scale intermittency of the velocity gradients organized by the individual main eddies and global intermittency associated with patchiness of turbulence on scales larger than the main eddies". In doing this, Mahrt (1988) described that physical properties of larger eddies in the boundary layer, not necessarily the stable layer, can result in smaller bursts of turbulence due to disruption of the mean atmospheric flow. Atmospheric data was then analyzed using the structure buoyancy length, defined by Mahrt (1988) as

$$d(r) = D_w{}^2(r)/\{\left(\frac{g}{\Theta}\right)[D_\theta{}^2(r)]^{\frac{1}{2}}\} \tag{1.3.3}$$

where w and θ are structure functions for vertical velocity, g the acceleration of gravity, and Θ the potential temperature. It was found that during times of strong stability, more of the variance of the data was found to result from intermittent extreme deviations from the mean, indicating possible turbulent bursting. However, Mahrt (1988) notes that this method does not necessarily describe the

characteristics of turbulence, but rather serves to describe the variance of the turbulence that occurs.

Chimonas (1998) takes a different approach to quantifying turbulent bursting events, by attributing them to step-like structures in the atmosphere that interact with existing waves, possibly resulting in increased shear and subsequent smaller-scale turbulence within the stable boundary layer. The step structures considered in the work were identified as the capping inversion at the top of the boundary layer and, when dealing with a heterogeneous surface, the shear layer occurring close to the ground (in this case, a forest canopy). Chimonas (1998) then describes internal steps within the stable layer as those that could possibly contain small-scale structures within themselves, such as layers possessing gravity waves (Figure 1.1). One major finding highlighted, however, was that when considering the eddy diffusivity in the stable layer was that it was much smaller than that found during the daytime convective, or mixed, layer, and was close in size to the value of molecular diffusivity of air (Chimonas, 1998). The main obstacle noted in the research was once again the lack of in-situ measurements. Furthermore, the measurements that had been obtained were not adequate enough to discern small scale turbulent structures with any measure of accuracy, and that before the turbulence can be understood the governing mechanisms of the stable layer and interactions with larger scale turbulence must first be determined.

In 1990, Nappo continued to move forward with research into turbulent bursting events by examining sporadic breakdowns in atmospheric stability over simple and complex terrain. One of the problems discussed was that when turbulence is averaged into boundary layer models, that fluxes of latent, sensible, and soil heat, along with net radiation are repeatedly underestimated. This underestimation in turn poses a problem when it comes to forecasting for the boundary layer. This occurs because vertical transfers in the stable layer are assumed to be small, and thereby given a constant value in most models, in turn not accounting for any bursting events that could modify transfers of heat or momentum. Upon further research, Nappo (1990) concluded that turbulent bursting occurs in the boundary layer not only over homogeneous terrain, but also heterogeneous, though there may be different triggering mechanisms in each case. It is also emphasized that the fact that models do not account for these events poses a serious problem for short-term air quality forecasting.

Coulter and Doran (2002) explored the spatial and temporal occurrences of turbulence using tower data collected during the CASES-99 campaign. The goal that was presented in their work was to identify triggering mechanisms for turbulent bursting, and the scale of these mechanisms, thereby discerning whether turbulence in the stable layer is localized at smaller scales, or spread out over larger scales. In order to describe the characteristics of turbulence, Coulter and Doran (2002) took the approach of analyzing 1-min vertical heat fluxes over

a night's worth of data, and discerned bursting events when the flux value would increase.

During the duration of their study, Coulter and Doran (2002) found that at each instrument location ranging from a 60m scaffolding tower and six surrounding 10-m satellite towers (Figure 1.2), there were roughly 4 to 7 events detected each night. They pointed out as well that windy nights provided less detected events, and also found that as height increases, the number of recorded events decreases, with the 20-m height acting as the boundary; with 5-6 events detected per night below the 20-m threshold, and 4-7 events per night above 20-m. Coulter and Doran (2002) did note, however, that the increase in magnitude of the vertical velocity must happen quickly, and exceed a given threshold value, which will be iterated further in future studies (e.g. Nakamura and Mahrt, 2005). One interesting finding, however, was that throughout the array of towers, events were detected at only certain locations, implying that turbulent bursting events in the stable layer have a relatively small horizontal extent. This methodology and corresponding results will be discussed in more depth in Chapter 5.

The relationship between the low-level jet, which tends to occur in mid-latitudes during the night has a significant impact on the stable nocturnal boundary layer, possibly being responsible for initiating turbulence at the top of the layer which can diffuse downward. Using data from a high-resolution Doppler lidar and data collected during the CASES-99 experiment, Banta et al. (2003) were able to examine the low-level jet, its properties, and turbulence kinetic

energy (TKE) in the stable boundary layer. Employing shear and stability estimates, Banta et al. (2003) came up with a modified form of the gradient Richardson number (1.3.4) , the bulk jet Richardson number (1.3.5), in order to sample turbulence and relate low-level jet properties to TKE characteristics.

$$Ri = \frac{g}{\theta}\frac{\Delta\theta/\Delta z}{\theta(\frac{\Delta U}{\Delta z})^2} \tag{1.3.4}$$

$$Ri_j = \frac{g}{\theta}\frac{\Delta\theta/\Delta z}{\theta(\frac{\Delta U_x}{\Delta Z_x})^2} \tag{1.3.5}$$

where U_x is the height of the first wind speed maximum in the layer and Z_x is the speed of the first wind speed maximum.

Analysis of the data shows when turbulence is present in the stable layer (as indicated by TKE values), plotted against values for Ri_j, that the total shear in the layer below the low-level jet tended to hover around a constant value of 0.1 s^{-1} (Figure 1.3). Banta et al. (2003) elaborates that this finding indicates that if stability of the atmospheric boundary layer, including energy and radiation budgets, were to be accurately calculated, that the value of Ri_j could then be discerned with fairly high confidence. Overall, the findings presented by Banta et al. (2003) serve to suggest that though this method works well for moderately stable boundary, that when considering the very stable layer, other factors such as the properties of turbulence must first be considered before Ri_j can be accurately calculated.

Another possible cause or turbulent bursting, as was previously discussed, is the passage of a density current. This cause is explored by Sun et al. (2002), once again relying upon data collected during CASES-99, and the use of High Resolution Doppler Lidar (HRDL) and a mini-sodar to monitor wind characteristic throughout the boundary layer. The method employed by Sun et al. (2002) was that to calculate turbulent fluxes from 5-minute means, which was felt to be adequate to sample most turbulent bursts over the duration of the experiment, and also short enough as to not capture mesoscale influences. During the night on 18 October 1999, a density current was observed to occur, identified by large temperature decreases across the tower, indicated by sonic anemometer data. Upon analyzing the observed frequency of the data, it was found that eddies were primarily responsible for the changes in temperature. Up to heights of 60-m, the temperature of the ambient air increased by ~3°C, and it was concluded that due to the frequency being greater than the Brunt Väisälä frequency, that gravity waves were not immediately responsible for the rapid temperature increase observed.

Flux measurements taken during the event indicated that the direction of moisture and carbon dioxide fluxes were downward, with sensible heat flux being upward. Sun et al. (2002) emphasizes this point since this behavior is opposite of the heat, moisture, and momentum fluxes observed in the ambient environment, depicted clearly in Figure 1.4. It was concluded that the density current created resulted in the creation of eddies, fueling the occurrence of

turbulent bursting in the layer, and further proved that mesoscale influences may be a cause for bursting events in the nocturnal SBL. This experiment will be discussed in more depth in Chapter 5.

In another study, Van De Weil et al. (2002) approached the problem of identifying turbulent bursting by classifying different nights during CASES-99 under one of three regimes: a turbulent regime, an intermittent regime, and a radiative regime. In order to classify the nights, a bulk model was used, and upon analyzing the equations and parameterizations employed in the model, a dimensionless number (Π) was found. Van De Weil et al. (2002) describe Π as being a function of outside forcing mechanisms, which impact the model and can be used to predict the state of the actual atmosphere, whether it be intermittent or nonintermittent.

After vigorous evaluations and comparisons between modeled data and observations during CASES-99, the three-regime classification was shown to be valid. Also, Van De Weil et al. (2002) found that mathematically stable nights and unstable nights were susceptible to being intermittently turbulent or continuously turbulent, respectively (Figure 1.5). This therefore furthers the validity of the Π parameterization in that it proves that turbulence can indeed be related to external forcing mechanisms, though the fixed shear assumption in the model equations must be addressed.

One additional experiment performed was that of Nakamura and Mahrt (2005), examining the occurrence of intermittent turbulence, once again, with

data collected during the CASES-99 campaign. Characteristics of turbulence, as described by Nakamura and Mahrt (2005), are that it must be suppressed below a threshold for time steps longer than the time it takes for a larger scale eddy to generate and dissipate, indicating that the burst is a structure of its own. Quantitative descriptions of intermittent turbulence are also given. One description is that provided by Nappo (1991) as described previously, that each period of wind speed and temperature covariance must exceed 10% of the mean to be considered an event. Howell and Sun (1999) took an approach that involved counting sub-periods of vertical heat flux that fit given criteria, and found that fewer sub-periods accounting for most of the fluxes indicated a larger degree of intermittency. This is similar to the method employed by Coulter and Doran (2002), as described before, when the goal was to identify certain periods with increased heat flux values. Finally, as described by Narasimha and Kailas (1989), a threshold value is used once again by Katul et al. (1994) to describe turbulent bursting in terms of the standard deviation of sensible heat flux.

Nakamura and Mahrt (2005) then defined their own coherent structure identification methodology, which involved calculating the variance of vertical velocity, and flagging the data set whenever a ratio of this variance exceeded a threshold value as being a bursting event. However, the threshold value used by Nakamura and Mahrt (2005), along with those used by Narasimha and Kailas (1999) and Katul et al. (1994) are all highly subjective, as are time

averaging intervals in other methods, both of which must be addressed before full understanding of the stable boundary layer and turbulence can be achieved.

Despite this, Nakamura and Mahrt (2005) found that during the CASES-99 experiment, that events occur less often when nights are weakly stable, or more windy, supporting the same conjecture made by Coulter and Doran (2002). It was also found that the turbulence events identified decreased with height over the time of observation (Figure 1.6). One main conclusion reached by Nakamura and Mahrt, however, is that given the resolution of instrumentation on the towers and data collected, the vertical scale of a bursting event is less than that of the tower height, allowing for the full amplitude of the burst to be measured using sonic anemometers looking at vertical velocities and corresponding variances. However, a concrete definition of what creates these events has not yet been achieved.

The focus of this research is to discern a robust coherent structure detection methodology, building upon that described by Nakamura and Mahrt (2005). By applying this new adaptive methodology, it is the goal to eliminate much of the subjective nature of existing techniques as described previously, such as threshold value and time average. Also, five main questions will be addressed:

1. Do turbulent bursting events and corresponding coherent structures exist in the Antarctic?

2. Can any causes of bursting in the stable layer be easily identified?

3. How does local stability play a role?

4. Can spectra analysis discern turbulent bursting events?

5. Is it possible to determine an objective technique for coherent structure detection?

In Chapter 2, a general overview of the characteristics of the Antarctic continent and corresponding persistently stable atmospheric boundary layer will be discussed. Following in Chapter 3, general information regarding boundary layer fluxes and their relation to Monin-Obukhov similarity theory will be described along with shortcomings of current atmospheric boundary layer models. Next, in Chapter 4, the ISCAT-00 campaign will be highlighted, and the data described in depth. Chapter 5 then will focus primarily on the details of the Nakamura and Mahrt (2005) coherent structure identification technique, corresponding findings, and a critique of the viability of the method as a whole, in addition to providing more information on selected existing methods. After describing the original detection method, Chapter 6 will briefly discuss the three datasets selected using the Nakamura and Mahrt methodology, followed by an in-depth analysis in Chapter 7, and analysis of the spectra of the datasets in Chapter 8. Chapter 9 will then serve to introduce the newly developed adaptive threshold technique and contain an analysis of the same three datasets for comparison to the Nakamura and Mahrt method, which follows in Chapter 10. Finally, in Chapter 11, a summary of the research will be provided, including the

answers to the five questions previously posed, and will touch briefly on future research directions.

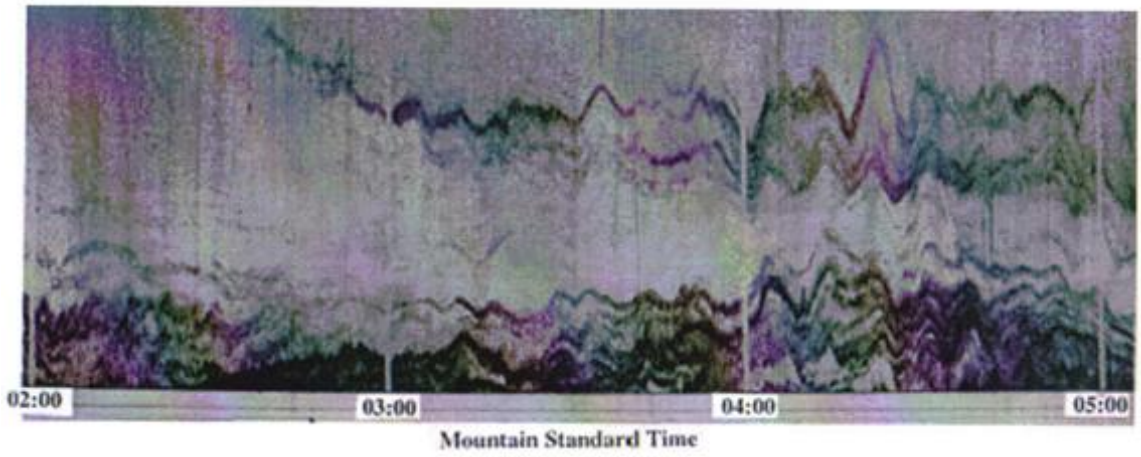

Figure 1.1: A depiction of a sounder record during a stably stratified night with gravity waves disrupting the laminar layer, Boulder (*image: Chimonas, 1998*)

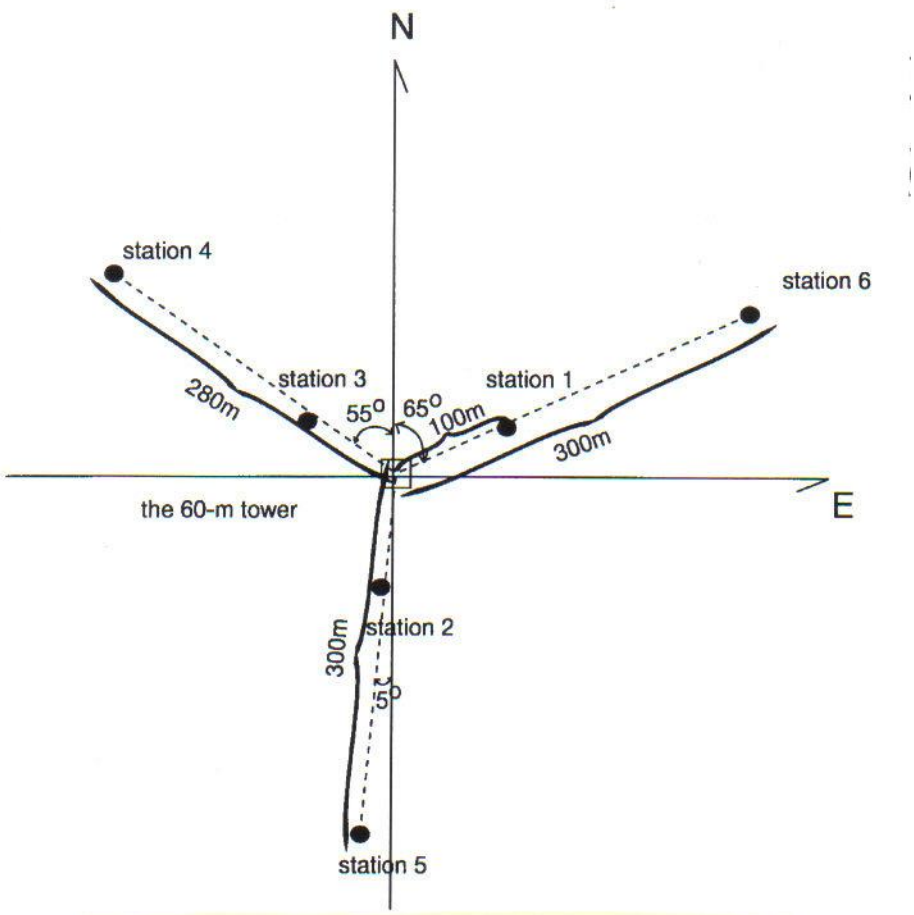

Figure 1.2: Overhead view of the layout of the CASES-99 tower array (*image: Sun et al., 2002)*

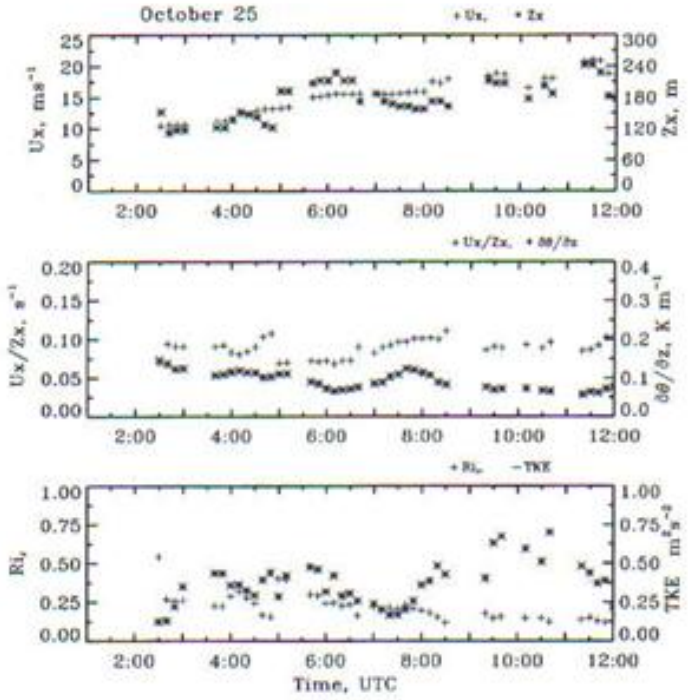

Figure 1.3: Low level jet characteristics in comparison to TKE values on the nocturnal boundary layer in mid latitudes (*image: Banta et al., 2003)*

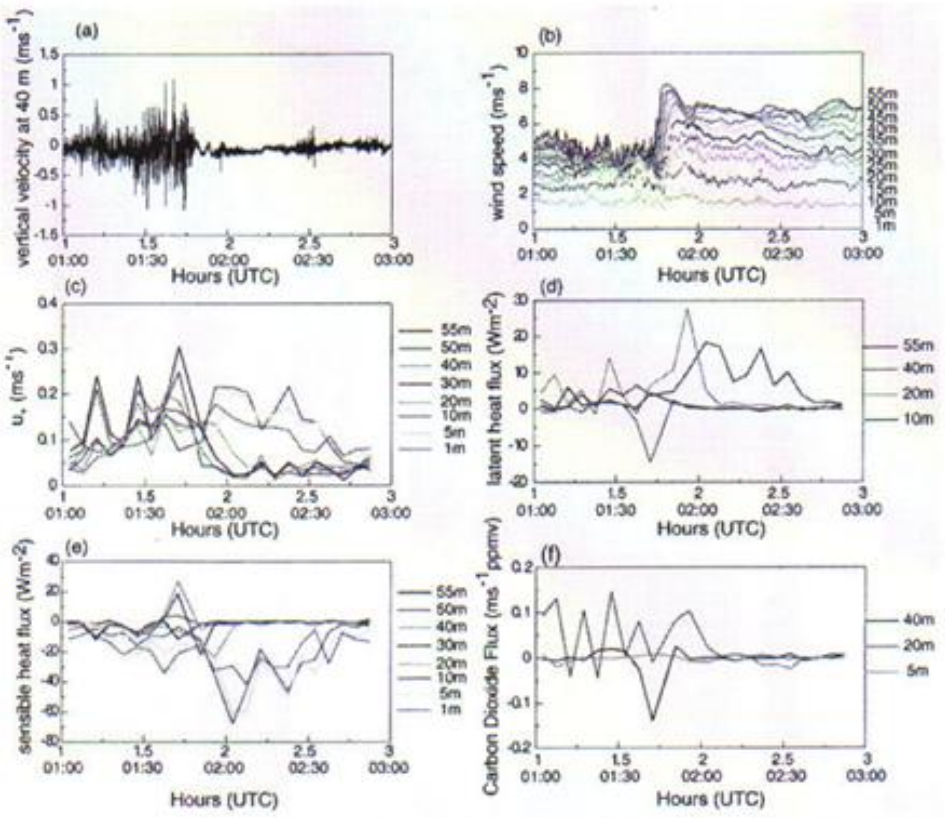

Figure 1.4: (a) time series of 40 m vertical velocity, (b) wind speed at different tower heights, (c) momentum transfer during density current passage, (d) latent heat during current passage, (e) sensible heat flux during current passage, (e) Carbon Dioxide flux during the current passage (*image: Sun et al., 2002)*

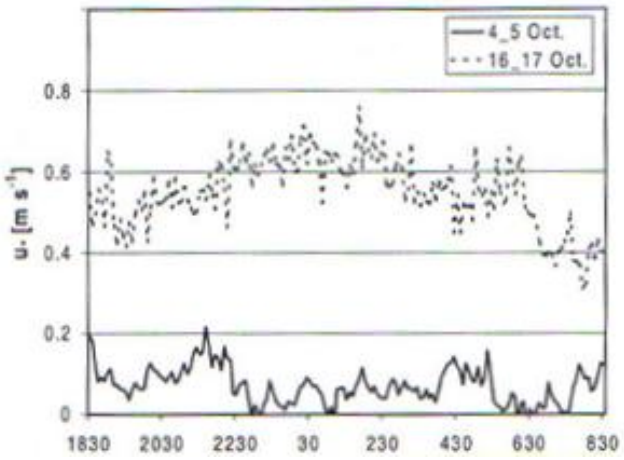

Figure 1.5: Comparisons between friction velocities on an intermittently turbulent night and a non-turbulent night (*image: Van De Weil et al., 2002)*

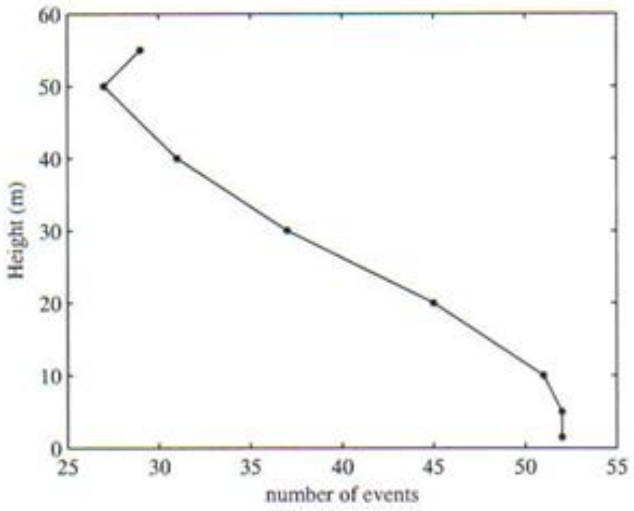

Figure 1.6: Number of events recorded during CASES-99 at different heights on the 60m tower (*image: Nakamura and Mahrt, 2005)*

CHAPTER 2

ANTARCTIC CHARACTERISTICS

2.1 Antarctic Topography and Atmospheric Characteristics

When considering the Antarctic surface layer, the topography of the Antarctic continent must first be discussed, given its uniqueness and the vast variation of elevations found to exist. As described by the *Antarctic Weather Forecasting Handbook* (hereafter, AWFH), Antarctica has a mean elevation of roughly 2000m, with most of the higher elevations confined to towering coastal mountain ranges and the east Antarctic ice sheet. A majority of western Antarctica is confined to low-lying ice sheets which extend inland toward 80° to 85° south latitude, typically with an elevation no more than 100m. Conversely, Dome A, located on the eastern Antarctic ice sheet, has a relative elevation of 4000m, which is equivalent to just over 13000ft. One of the most unique aspects of the Antarctic orography has to do, once again, with the coastal mountain ranges and the subsequent drastic increase in elevation over a short distance traveled inland. According to the AWFH, from 0° to 170° east longitude, it is not uncommon for the elevation to increase over 2000m within a distance of 400km from the shore. Furthermore, some of the coastal mountain ranges contain peaks that tower well above 3000m, rising from the low ice sheets below (Figure 2.1).

As is to be expected, this complex orography plays a very significant role in the weather patterns and general atmospheric flow around the region. The prevailing westerly winds observed to occur in midlatitude regions are found to extend toward the poles, and in the southern hemisphere, extend toward the Antarctic circumpolar trough. As described by the AWFH, the Antarctic Circumpolar trough is located in the vicinity of 63° south latitude in east Antarctica, and 68° to 70° south latitude in west Antarctica, with a notable discontinuity in the region around the Antarctic Peninsula, due to mountain ranges containing peaks that rise to well over 3000m.

Antarctica's continental asymmetry and climatological patterns of the ocean surface, including sea surface temperatures and the amount of sea ice, which is seasonally variable, are attributed to providing strong orographic and surface forcing to the circulation of the region, especially in conjunction with the Antarctic circumpolar trough. The AWFH expands on this, describing that seasonally, the wave pattern around Antarctica consists of 4 to 5 individual waves, but that the wave numbers may vary drastically by season. This is due in part to the seasonal changes in the amount of sea ice, with more waves occurring in the summer months when ice is reduced than in the winter months. Though, there is still variability even on an inter-annual time scale. There however tend to be several dominant low pressure centers that only vary slightly from season to season, as shown in Figure 2.2.

2.2 The Antarctic Boundary Layer

The Antarctic Boundary layer is different than that typically observed in mid-latitudes due to the fact that it does not vary drastically with the diurnal cycle. A general schematic of the mid-latitude boundary layer (Figure 2.3) depicts the diurnal variation due to solar radiation and cooling in mid latitudes. During the day, when solar insolation is at a maximum, the boundary layer is said to be convective, or well mixed. When the sun sets at the end of the day then, the heating source is thus removed, resulting in the formation of a new, stable layer that builds gradually upward from the surface throughout the night. It is in this layer that flux values reach a minimum, though immediately above this newly created stable layer, there remains a mixed layer, referred to as a residual layer, given that it remains from the afternoon's mixing. The diurnal cycle is then completed at sunrise, when solar insolation once again affects the boundary layer, serving to erode the nocturnal stable layer from the bottom up, replacing it with a new mixed layer as the day wears on. Through this, the lowest 1km of the atmosphere is typically what is examined for turbulence, which allows for the use of tower measurements in experiments such as CASES-99 (Coulter & Doran, 2002; Sun et al., 2002; Nakamura & Mahrt, 2005; and others).

However, a significant difference arises when considering the Antarctic boundary layer as opposed to the mid-latitude boundary layer. The main difference is that due to the lack of solar radiation received at the surface, resulting from the earth's tilt and the location of the Antarctic continent, that a

stable layer is almost always observed. The existence and persistence of the stable layer is encouraged by a lack of significant surface heating, which keeps the typically strong daytime fluxes of heat and momentum in the surface layer at a minimum, preventing the mixing of the atmosphere. Also, due to the snowpack and ice cover, the albedo of the Antarctic continent is very high, reflecting much of the solar radiation that manages to reach the area, allowing the stable layer to remain in place even during the Antarctic summer months. Furthermore, as shown in Figure 2.4, the process of layer breakdown that results in turbulence over Antarctica differs from that in mid-latitudes. This occurs primarily because when dealing with the persistent stable boundary layer, there is no residual layer remaining from during the day. Therefore, any disruptions in the flow or turbulent pockets that exist can move into the stable layer directly from the free atmosphere above, such as gravity waves or other larger-scale phenomena.

2.3 Antarctic Energy Exchanges

As was previously noted, the strongest stratification in the Antarctic boundary layer occurs during the winter months (June, July, and August), whereas the weakest, but still stable stratification occurs during the summer months (December, January, and February). Some of the first observations taken of the Antarctic surface layer were obtained and described by Hanson (1961). Using pyranometers and radiometers to measure solar and terrestrial radiation at several locations on Antarctica, providing estimations of the surface

fluxes and albedo during both summer and winter seasons, though I will focus on the summer season, given the data used in later sections. Hanson (1961) found that even though more solar radiation is received in Antarctica during the summer, that on average, the temperature remained around -27C in January, which on record tends to be the south pole's warmest month. Furthermore, despite there being 24 hours of sunlight at this time of year due to the earth's tilt and rotation, it was discovered that nearly 88% of the total incoming radiation (674ly. day^{-1} of 770ly. day^{-1}) is reflected from the high albedo snowpack and ice cover, while the difference was actually absorbed. However, this small amount of solar radiation was not enough to disrupt the layer, nor to increases the fluxes enough to begin any mixing actions above the surface.

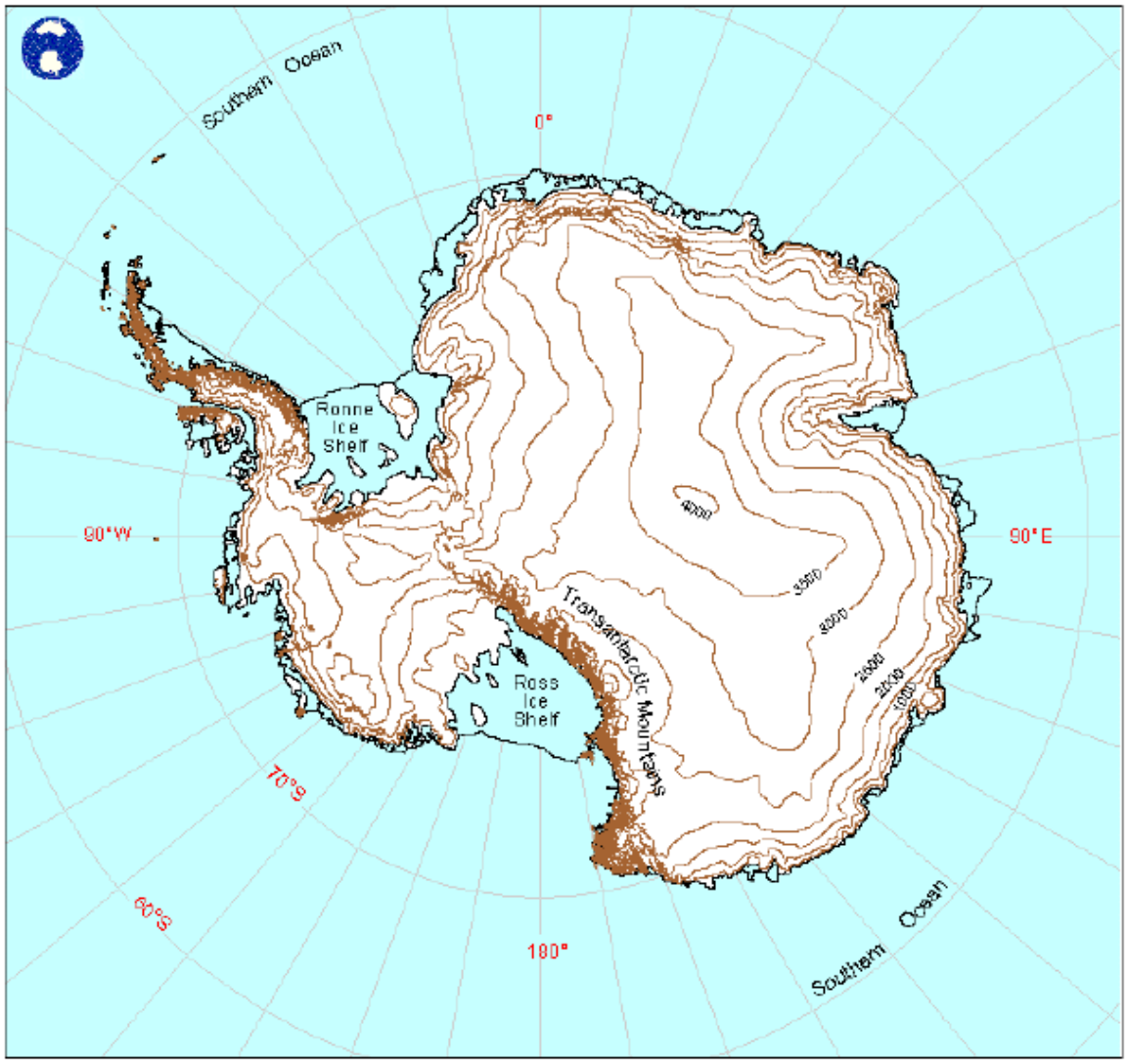

Figure 2.1: Orographic map of Antarctica, intervals of 500m (*image: Antarctic Weather Forecasting Handbook)*

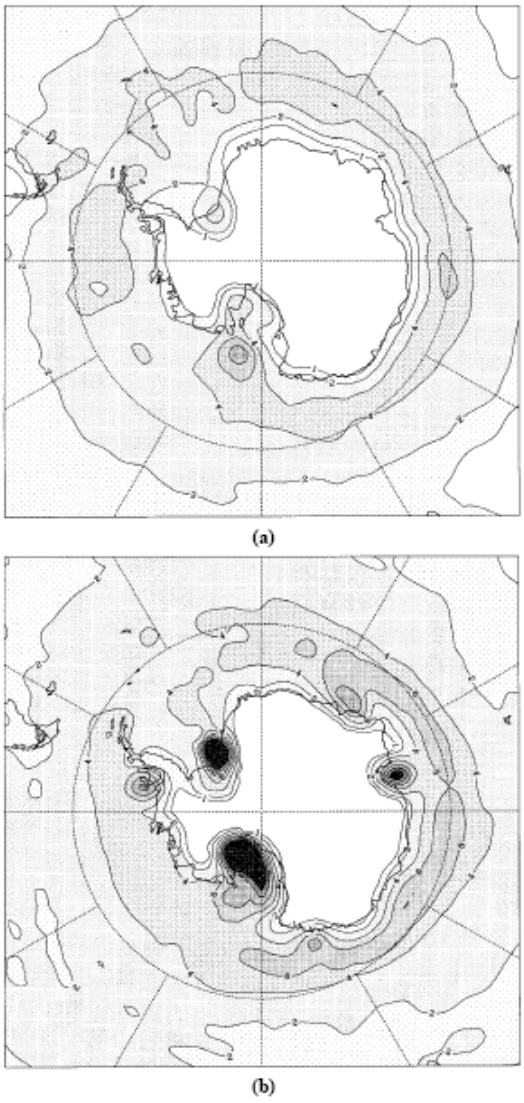

Figure 2.2: System density around Antarctica averaged yearly from 1958-1997, corresponding to low pressure centers in a) DJF (the Antarctic summer), and b) JJA (the Antarctic winter) (*image: Antarctic Weather Forecasting Handbook)*

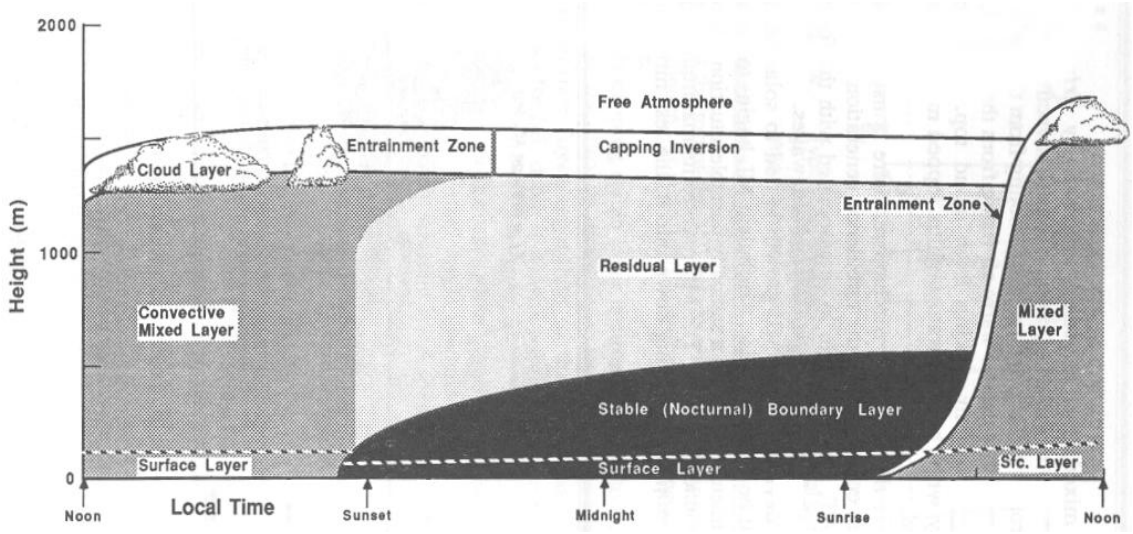

Figure 2.3: Diurnal diagram of the atmospheric boundary layer (*image: Stull, 1988)*

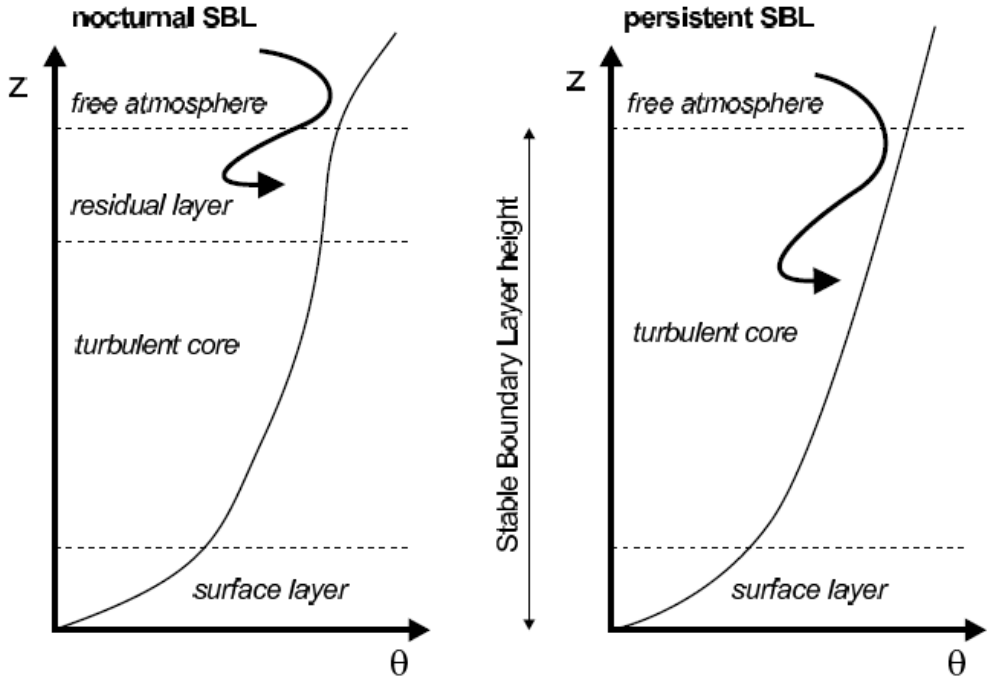

Figure 2.4: Transitionally stable nocturnal boundary layer versus persistently stable boundary layer (*image: Zilitinkevich, 2002)*

CHAPTER 3

ANTARCTIC BOUNDARY LAYER FLUX PARAMETERIZATIONS

3.1 General Flux Information

In 2000, Cassano et al. evaluated turbulent surface fluxes and parameterizations for the persistently stable boundary layer over Antarctica. However, upon comparing observed fluxes at the Halley, Antarctica observing site with those found using typical stable boundary layer model parameterizations, it was found that there was a major underestimation of downward sensible heat fluxes when applying the parameterized equations to a persistently stable regime. This could prove to be a significant problem for forecasting turbulence occurrences and their role in modifying the stable layer over Antarctica, given that it is these parameterizations that are employed in numerical models such as the National Corporation for Atmospheric Research (NCAR) Community Climate models CCM2 and CCM3, the fifth-generation Pennsylvania State University – NCAR Mesoscale Model (MM5), and the U.K. Met Office Unified Climate Model (UKMO) (The Antarctic Mesoscale Prediction System (AMPS), 2007). Furthermore, it was found that errors not only appeared in calculating sensible heat fluxes, but also low level wind speed and layer inversion strength and duration. Also, Cassano et al. (2000) found that problems in flux calculations could also arise from the simplicity that the parameterized equations are based on Monin-Obukhov similarity theory, and in this theory,

gravity wave influences are not taken into account, resulting in unphysical sensible heat flux values. Given that even the depth of the layer becomes a problem when applying typical model parameterized equations to the Antarctic, it is a necessity that a better understanding of Antarctic surface layer characteristics and momentum properties is gained before models can properly handle the persistently stable layer.

3.2 Identifying Stability Regimes from Boundary Layer Characteristics

One way that it is possible to discern stability classes in the boundary layer is by calculating the bulk Richardson number, given by Cassano et al. (2000)

$$Ri_g = \frac{gz(\theta_a - \theta_g)}{\left(\frac{\theta_a + \theta_g}{2}\right) V^2} \tag{3.1}$$

where g is the gravitational constant, z the height of the instrument, θ_a the potential temperature at the instrument height, θ_g the potential temperature of the surface, and V the value of wind speed. Cassano et al. (2000) continue to describe that it is possible to integrate dimensionless wind shear and temperature over a given height increment in order to parameterize the boundary layer, taking into account a stability correction function which can vary among any number of parameterizations considered. Figure 3.1 depicts a scatterplot of observed wind speed and low-level temperature inversion strength

using realtime data collected at the Halley site at a height of 4.5m with contours of Ri_g from 0.01 to 0.1 in steps of 0.01. This depiction allows for the identification of different stability regimes from the data, indicating periods of extreme stability to weakly stable conditions.

3.3 Weakness of Current Parameterizations in Stable Conditions

Sensible heat flux values exhibit the largest errors when calculating fluxes from data collected in the stable boundary layer. Cassano et al. (2000) outline the main cause for this as being the result of assuming that the surface scalar roughness length (z_0) is equal to the scalar roughness length (z_H). Using data collected at the Halley site, Cassano et al. (2000) found that in the Antarctic atmosphere, z_H is greater than z_0, which agrees with findings presented by King & Anderson (1994) though disagrees with Andreas (1987). Despite this, the results of Cassano et al. (2000) and King & Anderson (1994) allow improvement when applied to model parameterizations, and it is noted by Cassano et al. (2000) that since Monin-Obukhov similarity theory does not include gravity wave contributions to flux behaviors in the stable layer, that the larger z_H value can be used to account for the unrepresented range of heat flux values. The research presented in this thesis is expected to enhance understanding of basic boundary layer processes in the Antarctic, and in turn will hopefully help implicate more accurate model parameterizations for the stable boundary layer.

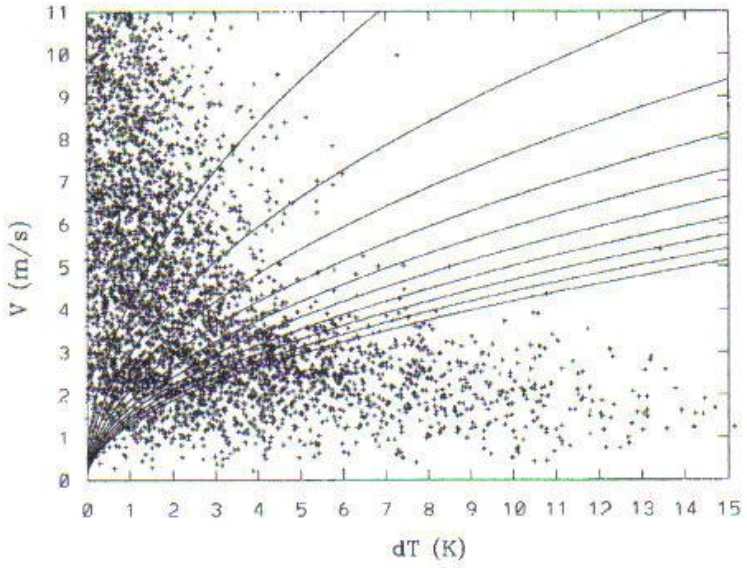

Figure 3.1: Observed wind speed (V) plotted against temperature inversion strength (dT) along with contours of bulk Richardson Number *(image: Cassano et al., 2000)*

CHAPTER 4

DESCRIPTION OF DATA

4.1 ISCAT 2000 Campaign

The data utilized in this research were obtained from that collected during the Investigation of Sulfur Chemistry in the Antarctic Troposphere (ISCAT) project which took place between 15 November and 31 December 2000. Though the primary scope of ISCAT 2000 was to explore the tropospheric chemistry in Antarctica as a follow-up to the previous 1998 study (Davis et al., 2004), the suite of meteorological instrumentation employed allowed for the collection of high resolution atmospheric data that could be used for boundary-layer turbulence research. These data were chosen to be utilized as the main focus of this research due to the fact that the atmospheric boundary layer in Antarctica is persistently stable. This, in turn, allows for a wide range of data over which to analyze and identify turbulent bursting events and coherent structures within the layer. Given that the primary focus of ISCAT 2000 was not atmospheric turbulence, but rather the fluxes of chemicals within the Antarctic troposphere, much of the instrumentation was employed in effort to establish chemical characteristics of the near-surface atmosphere and snowpack. Despite this, the use of sonic anemometers in order to estimate flux values proved to be beneficial when it came to examining variations in the vertical and horizontal velocities needed in order to positively identify turbulent bursting events in the stable layer.

The ISCAT 2000 campaign was conducted at the South Pole, at the Atmospheric Research Observatory (ARO) where a 22m meteorological tower (MET) was in operation with sonic anemometers at heights of 3.1 and 7.0 meters (Figure 4.1) above the snow-packed surface (Oncley et al., 2004). Also, there were temperature sensors located at 0.5, 0.9, 2.1, 4.7, 10.1, and 21.8m in order to measure potential temperature gradients, in conjunction with the sonic anemometers which served the primary purpose of measuring momentum and sensible heat fluxes, in addition to average wind and temperature.

One important aspect of the ISCAT 2000 campaign to note, however, is that it took place during the Antarctic summer, and during the summer, Antarctica receives more solar radiation, resulting in weaker stable boundary layers. However, as noted by Oncley et al. (2004), weather conditions during the first half of the collection period were fairly persistent, though toward the latter half of the sampling period, they became a bit more varied, primarily due to wind events. The most important meteorological variable to consider when examining atmospheric turbulence is the velocity field, and more specifically, the vertical component of the existing three-dimensional velocity vector.

However, important to note with this study, the quality and reliability of the data collected at the ARO MET tower are dependent on the direction of the mean wind. The ARO building at the South Pole is located at the apex of what Davis et al. (2004) noted to be the “clean air sector”, which simply means that it is located in an area that will remain uninfluenced by power generating facilities and other

man-made structures. This is important, because the fact that the MET tower and ARO building are upwind, it reduces the likelihood of man-made influences in the turbulence data. Furthermore, climatologically, the mean wind of the South Pole region falls within this “clean air sector”, which ranges from roughly 0-120°, and these winds also tend to be cooler and drier downslope flows as opposed to winds from other directions which are characterized as being warmer, moister, and primarily upslope flows (Davis et al., 2004). Davis et al. (2004) also expanded upon observed meteorological conditions and synoptic-scale flow patterns, and it and it was found that there were not any large-scale systems that could hinder the data from being used to examine stable layer turbulence.

Data were collected using the 3.1 and 7.0m sonic anemometers on the MET tower, given their capabilities to measure the three-dimensional velocity time series at a very high sampling rate, which, in the field of atmospheric turbulence, are most valuable. These raw data were collected at a 20 Hz sampling rate, compiled into text files including information on the horizontal and vertical components of velocity, temperature, pressure, and flux measurements, by the National Corporation for Atmospheric Research (NCAR). In order to use the data in this project, a graphical user interface (GUI) extraction module was employed (Figure 4.2), allowing for further adjustment of the full data set into smaller, more specific, more manageable files. The entire data set was then extracted in half hour increments, focusing entirely on temperature and the u, v,

and w components of velocity. Upon extraction, there was a need for rigorous quality control of the data set, which is discussed in section 4.3.

4.2 Measurement Issues and Considerations

When using instrumentation and data collected from instrumentation in order to estimate boundary flux values, certain aspects of the environment must be taken into consideration. This holds very true and is relevant to this research, in that the data analyzed are from an instrumented tower employing sonic anemometers and temperature and humidity sensors at varying heights. One major advantage of tower measurements as described by Dabberdt et al. (1993) is that due to the continuity of measurements, fluxes may be estimated from these data with more certainty that they are representative of the environmental fluxes in the immediate area.

Possible problems with data used from tower measurements, as noted by Dabberdt et al. (1993) include impacts of vertical advection, averaging time, stationarity, measurement height, site homogeneity, vertical alignment of the sensors, flow distortion, and shortcomings of the sonic anemometers themselves. First, vertical advection is not necessarily of concern when dealing with the persistently stable boundary layer, given vertical heat transport is at a minimum. Site homogeneity and measurement height tend to go hand-in-hand, with the required measurement height being a function of the amount of homogeneity observed over the site. The Antarctic Plateau allows for possibly

one of the most homogeneous surfaces that is observed, as it is relatively flat, and the snowpack uniform over the area. The only main drawback to the sonic anemometer is that the size and orientation of the instrument itself could result in flow distortion, however using new geometries; this problem has been alleviated, allowing the sonic to be used as the instrument of choice due to its rapid response, stable calibration, and linear output.

4.3 Quality Control Methodology

In order to alleviate some possible measurement errors as described in the previous section, rigorous quality control techniques were employed. As was noted previously, Oncley et al. (2004) described spiking problems with the 7.0m dataset in the latter half of the sampling period. This is a commonly encountered quality control issue, along with poor amplitude resolution, dropouts, and discontinuities in the data set (Mahrt and Vickers, 1996). Also, the first quality control method that had to be applied to each data set for analysis was a detrending technique, which simply allowed for the removal of larger scale wave patterns from the data set, leaving behind only the higher frequency portions of the set for further analysis. This removal of large-scale wave features from the data accounted for any corresponding large-scale atmospheric events, such as gravity waves, which could distort the turbulence time series. This was possibly one of the most important techniques employed, given the events of concern

were much smaller, harder to find coherent structures that could correspond to turbulent bursting events.

Despiking the 7.0m dataset was one of the primary tasks associated with the preliminary analysis of the dataset. As described by Mahrt and Vickers (1996), despiking can be accomplished using several simple steps to first detect spikes, then remove them, and then interpolate to fill in the "blanks" in the dataset. Though it was assumed that the spikes in the 7.0m data from the latter half of the sampling period were due to electronic problems with the sensor, but they could also be caused by precipitation events, or, as would likely be another possible scenario in Antarctica, wind transporting ice crystals onto the sensors.

The first step toward spike detection was identifying a standard deviation threshold, and depending on how many points exceeded this threshold using a series of moving windows, the data may be flagged as being a spike. If a spike were to be identified, linear interpolation would be used to replace it. The second step, as described by Mahrt and Vickers (1996), was to use an iterative method for spike detection, increasing the standard deviation by 0.1 on each successive pass. Once the number of spikes replaced in the data set exceed 1% of the total number of data points (36000 in this instance, per each half-hour increment), the set is indicated as being despiked (Figure 4.3 provides an example of despiking using the Mahrt and Vickers technique). However, Mahrt and Vickers (1996) note that the choice to use a specific window size, the 3.5 standard deviations threshold, the increasing standard deviation increment of 0.1, the limitation of

events to be 3 or fewer points, and the 1% criteria are arbitrary and subtle changes here can in turn affect the final dataset. However, upon employment of this method with regard to the 7.0m data, it appeared to work very well and fit the needs of the set, and thus was not further modified in any fashion for this study.

Another potential problem with any dataset collected, especially from a tower and with the goal of examining atmospheric phenomena is that of amplitude resolution. Since the focus of this research is the stable boundary layer, it is expected that there would be weak winds, and corresponding weak variance within the dataset itself. The problem that arises here, then, is that the amplitude resolution of the recorded data may not be sufficient to capture the fluctuations in the dataset, therefore yielding a misinterpreted set. In order to detect a possible amplitude resolution issue, the turbulence time series were visually inspected for any amplitude resolution errors or data dropouts, problems described in Mahrt and Vickers (1996).

All things considered, however, the ISCAT-00 data set was found to be highly beneficial to this research. After employing the quality control methodologies outlined by Mahrt and Vickers (1996) and a simple detrending technique (Basu et al., 2006), the resulting time series of vertical velocity obtained from the sonic anemometers at both 3.1m and 7.0m were able to be further analyzed to determine the existence of turbulent bursting events and corresponding coherent structures.

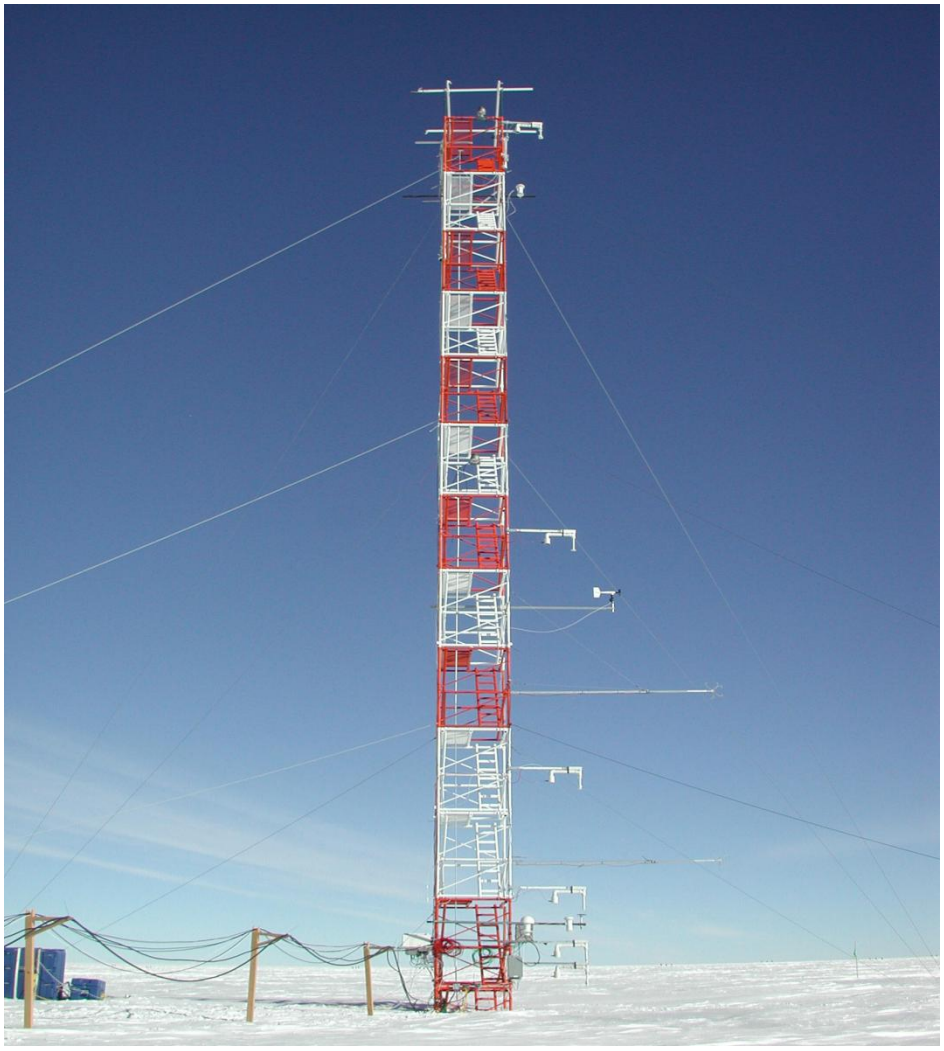

Figure 4.1: Instrumented ISCAT-00 tower in Antarctica (*image: NCAR)*

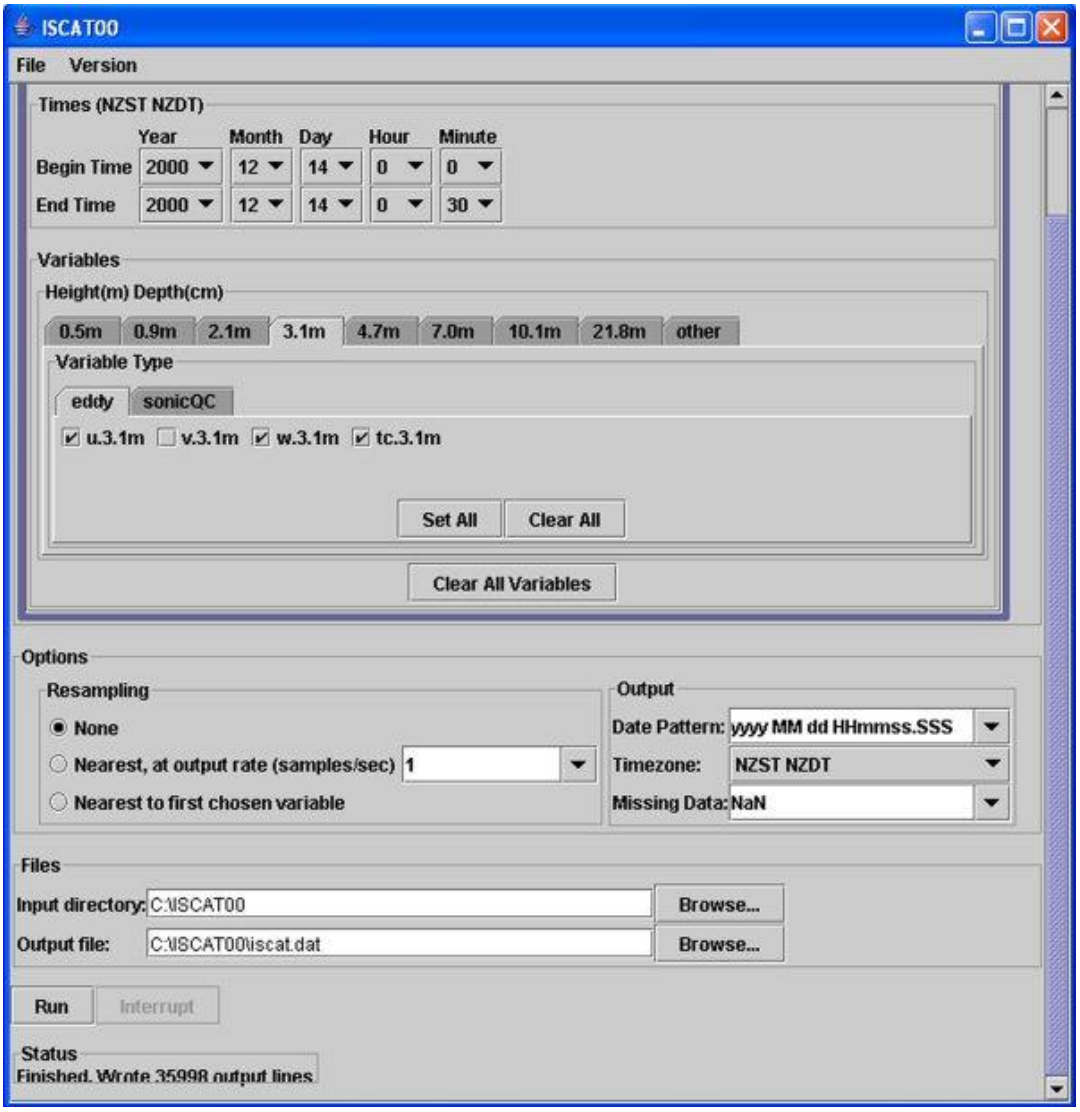

Figure 4.2: GUI used in order to extract the ICSAT-00 data in half-hour increments

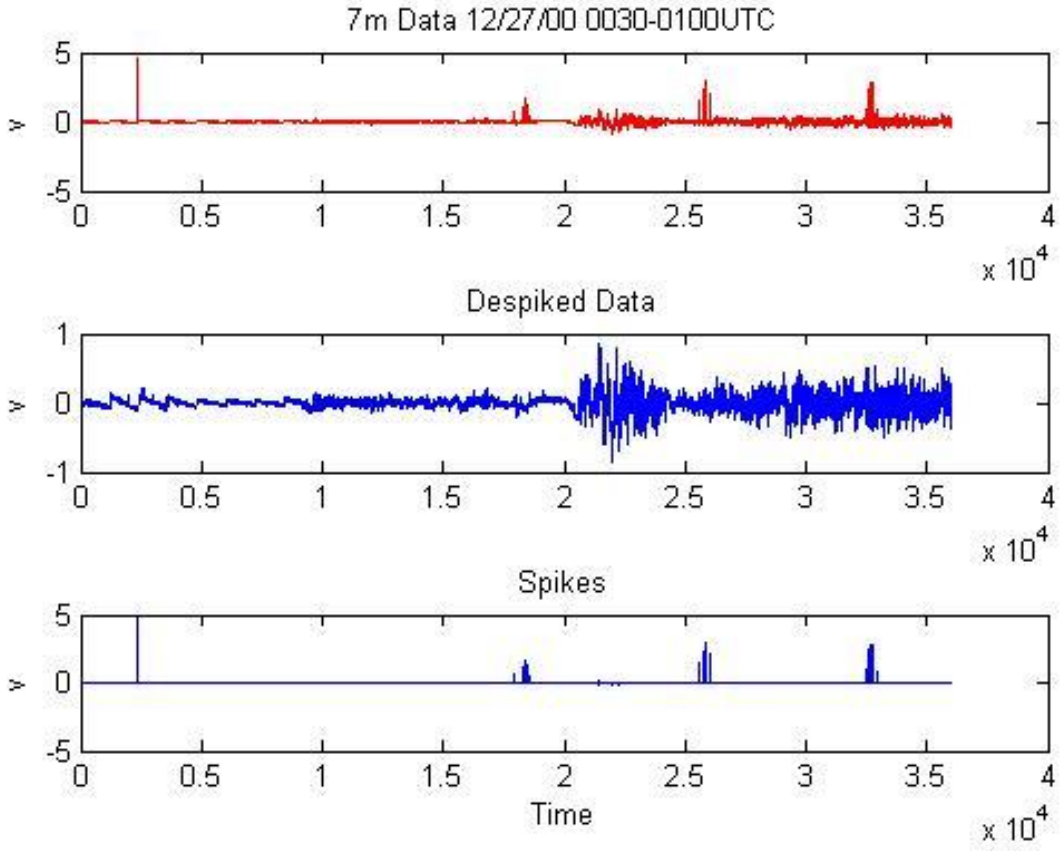

Figure 4.3: Example of despiked ISCAT-00 data. The original signal is shown at the top, the signal with spikes removed in the middle, and the spikes themselves are plotted on the same time scale in the bottom frame.

CHAPTER 5

EXISTING COHERENT STRUCTURE (BURSTING) DETECTION METHODOLOGIES

5.1 Previous Turbulent Bursting Studies

Though not much is currently known about the origins of turbulent bursting events, it has been a topic of interest to researchers for the better part of the last 40 years. As described by Narasimha and Kailas (1989), Kline et al. (1967) was first to identify the turbulent burst as "a coherent quasi-periodic cycle of events occurring in the boundary layer". Narasimha and Kailas (1989) felt that the best way to identify the events by examining instantaneous flux values, and look closer at certain times when the flux has significantly larger values than others. Using data that were collected on 11 September 1978 from a tower in Boulder, Colorado, they were able to compare with existing tower results and found that both sets of data not only had similar features, but that bursting events can have a mean flux over a very small time frame nearly 10^6 to 10^9 times larger than that of the molecular transport. Narasimha & Kailas (1989) employed the VITA technique (Narasimha & Kailas, 1987), which was successfully used to take a closer look at a turbulent quantity over a short time variance (discussed in more depth in Section 1.3). Narasimha & Kailas (1989) do point out, once again, that the events depend on the averaging time used, along with the threshold value, both arbitrary constraints. In previous work (e.g. Kailas & Narasimha, 1988), it

was found that depending on the flow, the time averaging value could range anywhere from 1s to 10s, and was found to still apply to both datasets that were being examined. In this experiment, it was also started for clarification's sake that a burst is a coherent event in itself, which can be comprised of several neighboring ejections from the same initiation point, as opposed to the smaller ejections themselves. Also, Narasimha & Kailas (1989) pointed out that once the time averaging value exceeded 10s, the frequency of detection of events for u', v', and w' all became independent of the time frame used.

Much of the research completed regarding turbulent bursting events used data collected from CASES-99, an experiment conducted on the plains of Kansas using an array of 10m instrumented towers surrounding a larger 60m instrumented tower (refer to Figure 1.2). The primary benefit of this experiment was a large sampling area, and the ability to capture bursting events on different time scales and perhaps sample propagation rates from tower to tower. One such analysis was performed by Coulter & Doran (2001), who considered fluxes to be the best indicatiors of a turbulent bursting event. First, flux values were calculated over a 1 minute interval, and after a smoothing technique was applied, the average 12 hour fluxes could be obtained. This analysis was performed for all instruments, and over six stable nights, and two weakly stable nights in order to compare flux values and wind speed and direction. After comparison, Coulter & Doran (2001) found that turbulent fluxes remained very small throughout the night, though when these fluxes increased due to turbulence, they were 1.5 to 2

times larger than the average. Also, it was found that with increasing stability, the majority of energy transfer tends to occur sporadically in conjunction with identified bursting events, as opposed to the weakly stable nights, where energy transfers tended to occur gradually over the duration of the night.

In addition to the characteristics of the events, Coulter & Doran (2001) also explored the correlations between events at different heights over the instrumented towers, and also over distances between the towers in the CASES-99 array. It was found that correlations between events are more commonly found at towers in close range of one-another, as indicated by a burst having the same characteristics at one tower from 0230 to 0330 as a burst at a nearby tower from 0300 to 0400 the same night. Also, Coulter & Doran (2001) found the existence of events at two levels over the same instrumented tower, though this occurred less often during stable nights than weakly stable nights.

Another experiment using CASES-99 data was performed by Sun et al. (2002), and in order to identify the occurrence of stable boundary layer turbulence, a case involving the passage of a density current was examined. In addition to using the collected tower data, Sun et al. (2002), as discussed previously, employed the HRDL and the Argonne National Laboratory Boundary Layer Experiment (ABLE) Doppler mini-sodar in order to monitor wind profiles and corresponding radial velocities and their roles in turbulent bursting events. The method used by Sun et al. (2002) involved calculating turbulent fluxes from 5

minute means of the original data set, and the intervals that were used were chosen to be void of mesoscale influences, to ensure maximum stability

5.2 Nakamura and Mahrt (2005) Coherent Structure Detection Technique

Nakamura and Mahrt (2005) first defined intermittency as requiring that "the turbulence is partially suppressed below some small threshold for periods much longer than the time-scale of the individual main eddy". They also noted that earlier Nappo (1991) described that fewer intermittent turbulent events were identified as the duration between events increased. Their work consisted of an investigation of CASES-99 data, and identifying intermittent turbulent events using two specific criteria. Using vertical velocity perturbation data, an event onset would be defined as when the magnitude of the vertical perturbations increase quickly, and also, not only would this velocity have to increase, but it would also have to surpass a given threshold value.

In order to identify these onsets and extract them from the background data set, Nakamura and Mahrt (2001) first divided up the vertical velocity data into a pair of non-overlapping 5 minute windows, which could be advanced forward in time steps relevant to the data being analyzed. Within each of these 5 minute windows, the vertical velocity data was detrended, allowing for the removal of larger-scale wave-like structures that could be due to outside influences such as gravity waves or resonating effects from a previously occurring weather system earlier in the day, leaving behind only the higher

frequency velocity data. The first step to their coherent structure detection methodology was then to calculate the radio of increase of vertical variances between each window in order to come up with a value for the Turbulence Enhancement Index (TEI) (5.2.1).

$$TEI = \frac{\overline{w'_2{}^2} - \overline{w'_1{}^2}}{\overline{w'_1{}^2}} \qquad (5.2.1)$$

Each window was chosen to have a width of 5 minutes, because it was felt that this window size was not only long enough to identify intermittent turbulent events, but was also short enough so that any remaining larger-scale wave features that were not removed by the initial detrending would not be captured in the variance calculations (Nakamura and Mahrt, 2005). After this is completed, each set of windows is advanced through the data set in 10 second increments until the entire set has been covered.

After the preliminary analysis is complete, and the TEIs have been calculated for each series of windows, the TEIs are put into descending order, and whenever the TEI value exceeds a given threshold (defined as 3, by Nakamura and Mahrt, (2005)), the onset of an event is defined. However, the onset is only valid if it is defined not within 5 minutes of another onset, in order to prevent 'double counting' of a single event. However, it is important to note, that both the value of 3 for the TEI threshold and the idea that 5 minutes is adequate time for an event to initiate and dissipate are very much arbitrary. Nakamura and Mahrt (2005) touch on this aspect briefly, by discussing that when the threshold is

decreased from 3 to 2, that there are more events defined, and conversely, less are defined when the threshold is increased from 3 to 4.

5.3 Coherent Structure Identification Method Limitations

In all the previous cases discussed, not only in Nakamura and Mahrt (2005), but also in Coulter and Doran (2002), Sun et al. (2002), and Narasimha and Kailas (1989), one problem appears to arise in each coherent structure detection methodology. This problem is that of subjectivity. Nearly every method uses a time window, however, this window between the reviewed literature varies anywhere between 1 second and 5 minutes, and in each investigation, the choice for the time window duration is validated and shown to be useful for the analysis at hand. Furthermore, as was previously mentioned, the Nakamura and Mahrt (2005) methodology is highly subjective. First, since there is no concrete definition of these coherent bursting events, it cannot be known for certain whether 5 minutes is adequate allotment for an event to initiate and then dissipate back to a fully stable regime. Also, Nakamura and Mahrt (2005) note that the threshold value, as it is increased or decreased, affects the number of onsets defined. Intuitively, it can also be expected that as the window size of 5 minutes is either lengthened or shortened, even keeping the threshold at a constant value, the number of onsets would be altered. So, the main problem with existing coherent structure identification methodologies is not that they are

not valid or accurate, but rather that the validity of the analysis is impacted by subjective choices of important threshold and time window values.

In Chapter 6, I propose a new coherent structure detection method, which builds upon the pre-existing Nakamura and Mahrt (2005) coherent structure detection technique. The new method will serve to remove much of the subjective nature of the analysis by using a newly developed adaptive threshold methodology, and in turn, provide a more robust way of approaching the problem of identifying not only the onsets of these bursting events, but of characterizing the events themselves.

CHAPTER 6

ANALYSIS AND FINDINGS USING THE NAKAMURA AND MAHRT COHERENT STRUCTURE DETECTION TECHNIQUE

Using the Nakamura and Mahrt (2005) coherent structure detection methodology, as outlined in the previous chapter, there were 21 half-hour increments during ISCAT-00 identified as containing the onset of a turbulent bursting event (Table 6.1). In employing the use of this methodology, the guidelines outlined in Nakamura and Mahrt (2005) were strictly followed, using a time averaged window of 5 minutes and a threshold value of 3. Interesting to note is though there were 21 individual cases identified at 3.1m and 7.0m heights, of these 21, there were three instances where the onset of bursting was identified at both 3.1m and 7.0m, indicating the variation of vertical extent between such events. In other cases, the event was indicated at only 7.0m, or only 3.1m.

After all the data was analyzed using the method developed by Nakamura and Mahrt (2005), three sets were selected for further examination and testing using a newly developed adaptive threshold methodology as described in Chapter 9. These three cases chosen were 24 December 2000 during the half hour period between 0630 and 0700 New Zealand Daylight Time (NZDT), 27 December 2000 between 0030 and 0100 NZDT, and 28 December 2000 between 0630 and 0700 NZDT. The first two cases (hereafter Case 1 and Case

2, respectively) were found to have onsets indicated at both 3.1m and 7.0m. Conversely, the third case chosen (hereafter, Case 3), contained a bursting onset identified only at the 7.0m height. In further analysis of these events, the respective time series will be analyzed beginning one hour before the half-hour increment of data where an onset was defined, and one hour after this time period, in hopes of capturing the full set of characteristics over lifetime of the turbulent burst.

Table 6.1

Date	Time	Event Detected At 3.1m	Event Detected At 7.0m
15 December 2000	1030-1100 NZDT	Y	N
15 December 2000	2000-2030 NZDT	N	Y
16 December 2000	0000-0030 NZDT	N	Y
23 December 2000	1600-1630 NZDT	Y	N
23 December 2000	1800-1830 NZDT	Y	N
24 December 2000	0430-0500 NZDT	N	Y
24 December 2000	0600-0630 NZDT	Y	N
24 December 2000	0630-0700 NZDT	Y	Y
24 December 2000	0930-1000 NZDT	Y	Y
25 December 2000	0100-0130 NZDT	N	Y
25 December 2000	0200-0230 NZDT	N	Y
27 December 2000	0030-0100 NZDT	Y	Y
27 December 2000	2330-0000 NZDT	N	Y
28 December 2000	0230-0300 NZDT	N	Y
28 December 2000	0330-0400 NZDT	N	Y
28 December 2000	0400-0430 NZDT	Y	N
28 December 2000	0630-0700 NZDT	N	Y
28 December 2000	0700-0730 NZDT	N	Y

CHAPTER 7

METEOROLOGICAL CHARACTERISTICS AND FLUXES ASSOCIATED WITH TURBULENT BURSTINGS

7.1 Synopsis of Meteorological Conditions

In order to answer the first question posed, regarding whether micro/mesoscale meteorological conditions were able to explain the occurrence of such bursting events, the three events were examined, and compared, in order to see if there were any striking similarities. Figures 7.1, 7.2, and 7.3 depict the findings of Case 1, Case 2, and Case 3 respectively. In each plot, the red line depicts data collected using the 3.1m sonic anemometer, and blue the data collected using the 7.0m sonic anemometer. First, wind speed (M) and wind direction (D) are plotted, in addition to individual plots of vertical velocity (w) for each height, sampled at 20Hz. Then, the pressure tendency (P) is plotted, sampled at 1Hz, and finally, the acoustic virtual temperature (T_C) as indicated by the 20Hz sonic anemometers is plotted for both heights.

The first similarity between the three cases of bursting to note is the continuous increase in pressure preceding and after the event onset was indicated to have occurred. In all three cases, the increase in pressure is gradual, and does not seem to have any sudden, marked increases, so it is difficult to discern whether this increase played a part in initiating the turbulent burst, or if it was a result of a larger scale phenomenon that later impacted the

turbulent bursting characteristics. Another similarity between the cases is that in all three, an increase in wind speed was experienced around the time of bursting onset, only around 1 m s^{-1} in Case 1, though much greater in Case 2, nearly 3 m s^{-1}, and 2 m s^{-1} in Case 3. However, in Case 3, the velocity continued to fluctuate, whereas in Cases 1 and 2, the increase remained fairly consistent during the time of onset identification. Also, a significant change in wind direction was observed in addition to a wind speed increase for Cases 1 and 2. In Case 1, the wind shifted from ~90° to ~20°, corresponding with the increase in wind speed. Case 2, however, exhibited the most significant direction change, shifting ~120° nearly suddenly, at the same time the winds increased by 3 m s^{-1}, corresponding with the onset of the burst.

Due to the wind speed increases and direction changes observed in Cases 1 and 2, it can be assumed that the bursting identified in these cases is due to wind shear at low-levels. Since the wind speed in both cases remained higher at 7.0m, directional shear could have resulted in enough disruption in the stable layer to cause turbulence to occur. Also, the direction change experienced at both heights during both events indicates shearing instability, though the direction change in Case 1 is slightly greater at 3.1m, indicating the possibility that the turbulence could have propagated upward. In Case 2, the direction change is fairly consistent at both heights. Sun et al. (2002) discusses the possibility of turbulence generation due to a pressure change, which can possibly serve to explain the occurrence of the bursting event identified in Case

3, and possible impacts on the events in Cases 1 and 2 in addition to wind shear. However, as Sun et al. (2002) points out in their turbulence study, the pressure had been decreasing prior to the event, which is not observed over the time scale of this analysis. Despite this, the gradual increase in pressure coupled with the increases and variation in wind speed could be enough in this case to cause turbulent bursting.

For further consideration, Case 2 was chosen for analysis using the Antarctic Mesoscale Prediction System's Weather Research and Forecasting model (AMPS WRF) in order to examine meteorological conditions over a larger scale, to be sure that no large scale disturbances were in the vicinity. The importance of finding out conditions at larger scales in the atmosphere at the time of the event has to do with classifying the event as a true turbulent burst, and ruling out possible large-scale influences such as a density current or katabatic wind event. The AMPS WRF configuration used was that of a triply nested grid (60km/20km/6.67km), centered over the ISCAT-00 tower location. The grid dimensions were 127 grid points in the x-direction, 127 grid points in the y-direction, and 31 vertical levels. The model was initiated 24 hours prior to the event of interest, and was allowed to run until 12 hours after the event, allowing for adequate spin up and realization of atmospheric variables. Meteorological conditions plotted included 500mb vorticity, 300mb, 500mb, 700mb, 850mb heights, winds, temperature, and humidity, accumulated precipitation, and a general surface analysis of pressure, winds, temperature, and humidity.

First, examining large-scale data, there were no localized vorticity maxima over the area during the time of the event, and no large-scale temperature gradients leading to any advection, as one would expect to see at multiple levels if a larger, synoptic-scale system were progressing through the area. Figure 7.4 (a - d) depicts the WRF simulated conditions at the surface (temperature, dew point, winds, and pressure) over the area during the time of the turbulent event, and important to note first are that the winds at 20 minute intervals never change direction, nor do they change magnitude, remaining at a relatively calm 10 knots. The temperature remains fairly constant as well, and there are no indications of a tight temperature or pressure gradient, which would be indicative of some sort of frontal passage. Also, there were no apparent large-scale causes for the burst to occur at the time it was observed, the winds staying in the same direction, at a relatively calm overall speed around 10 knots, overruling the possibility of a katabatic wind event or associated gravity wave phenomena.

Interesting to note, however, is that despite the fairly consistent atmospheric conditions at the time, changes in potential temperature at all levels on the ISCAT-00 tower are found to have occurred at the time immediately preceding the turbulent burst as identified using the Nakamura & Mahrt (2001) method. Figures 7.5, 7.6, and 7.7 depict this potential temperature change for Case 1, Case 2, and Case 3 respectively, in a time-height plot created from temperature data collected from 1Hz slow response temperature sensors at 0.5, 0.9, 2.1, 4.7, 10.1 and 21.8m levels. Pressure measured at 1m was then used

to calculate the potential temperature after using the hypsometric equation to estimate pressure values at the same temperature heights. In Case 1 a, a significant increase in potential temperature is observed, compared to that in Case 3, which is a much more subtle potential temperature increase. Case 2, on the other hand, displays a significant, fairly rapid decrease in potential temperature corresponding to the onset of the turbulent burst. At this point, it is unclear whether this change in potential temperature was an indicator of the onset of the event, or rather a possible catalyst of the event's occurrence.

Overall, after examination of meteorological conditions over the ISCAT-00 site, it can be concluded with confidence that indeed this event was not the result of a large scale atmospheric feature, and thereby can be further studied using coherent structure detection methodologies in hopes of discerning the characteristics and possible causes of the event to occur.

7.2 Observed Fluxes

A further step that can be taken when analyzing boundary layer characteristics, is to consider the fluxes that exist. One way to take these fluxes into consideration is to compute the Monin-Obukhov length scale, which indicates the height at which mechanically generated turbulence is in balance with the overall dissipative effect. Vandop (2007) gives this equation as

$$L = -\frac{{u_*}^3}{\kappa\left(\frac{g}{T}\right)\overline{w\theta_o}} \tag{7.1}$$

where L is the M-O length, u_* is the friction velocity, and κ the Von-Karman constant (0.4). When concerning atmospheric stability and turbulence, the main three scales to focus on are L, z/L, and u_*, and in cases of instability, z/L is expected to be less than zero, and friction velocities larger.

Upon analysis of the ISCAT-00 tower data, results were found that were very clearly consistent with those expected in a stable environment, as depicted in Table 7.1. Friction velocities remain small, as the surface at the site is relatively homogeneous, flat terrain; z/L remains positive, indicating stable stratification in the boundary layer; and L decreases (z/L increases) with height as typically observed in the stable boundary layer.

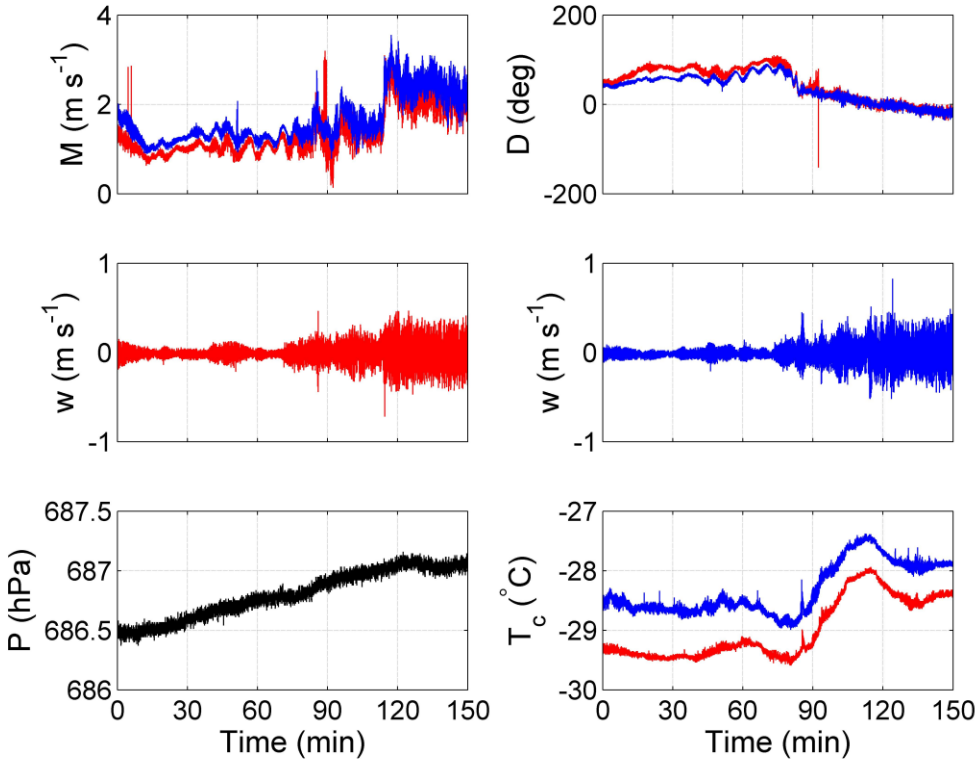

Figure 7.1: Wind speed, wind direction, vertical velocity, pressure tendency, and acoustic virtual temperature plotted for both 3.1m (red) and 7.0m (blue) for Case 1.

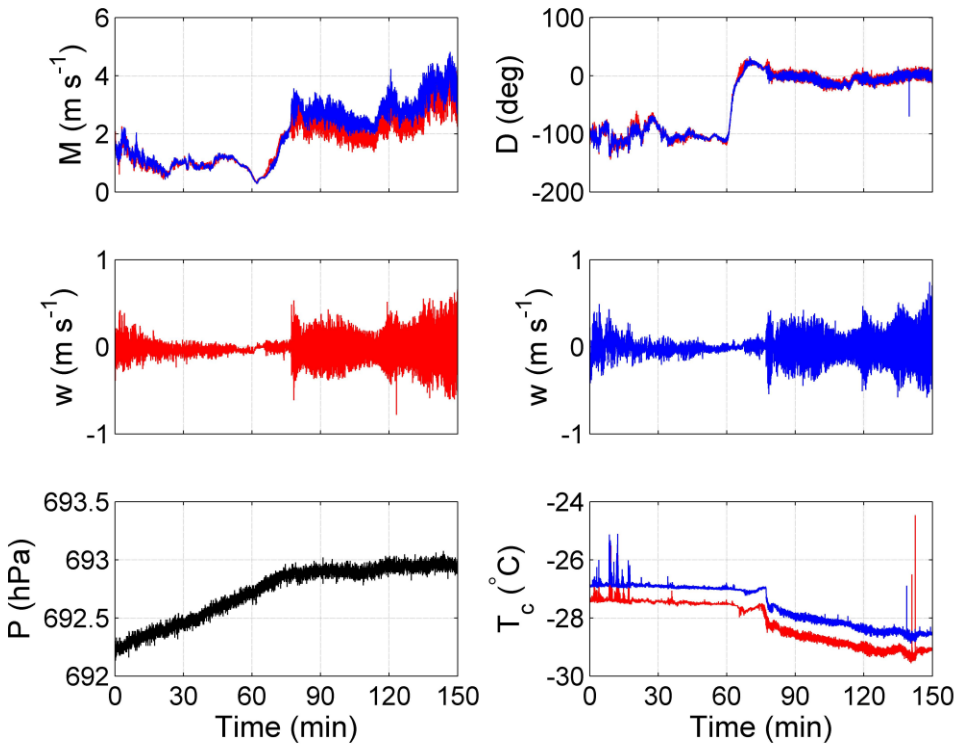

Figure 7.2: Wind speed, wind direction, vertical velocity, pressure tendency, and acoustic virtual temperature plotted for both 3.1m (red) and 7.0m (blue) for Case 2.

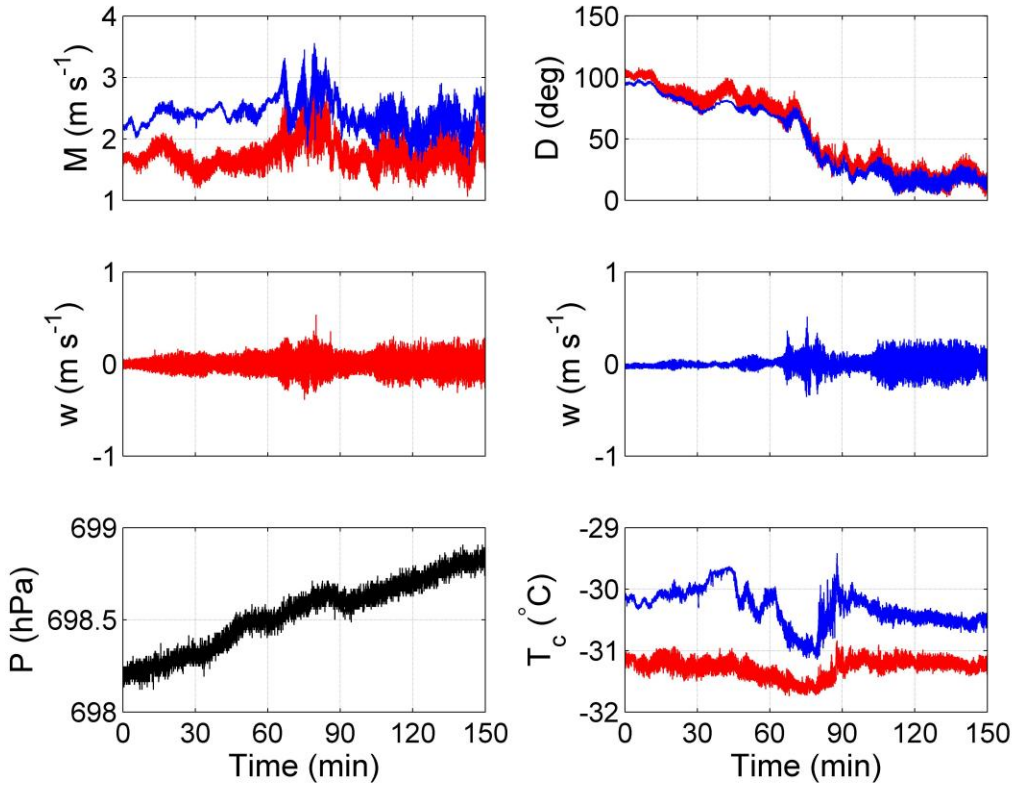

Figure 7.3: Wind speed, wind direction, vertical velocity, pressure tendency, and acoustic virtual temperature plotted for both 3.1m (red) and 7.0m (blue) for Case 3.

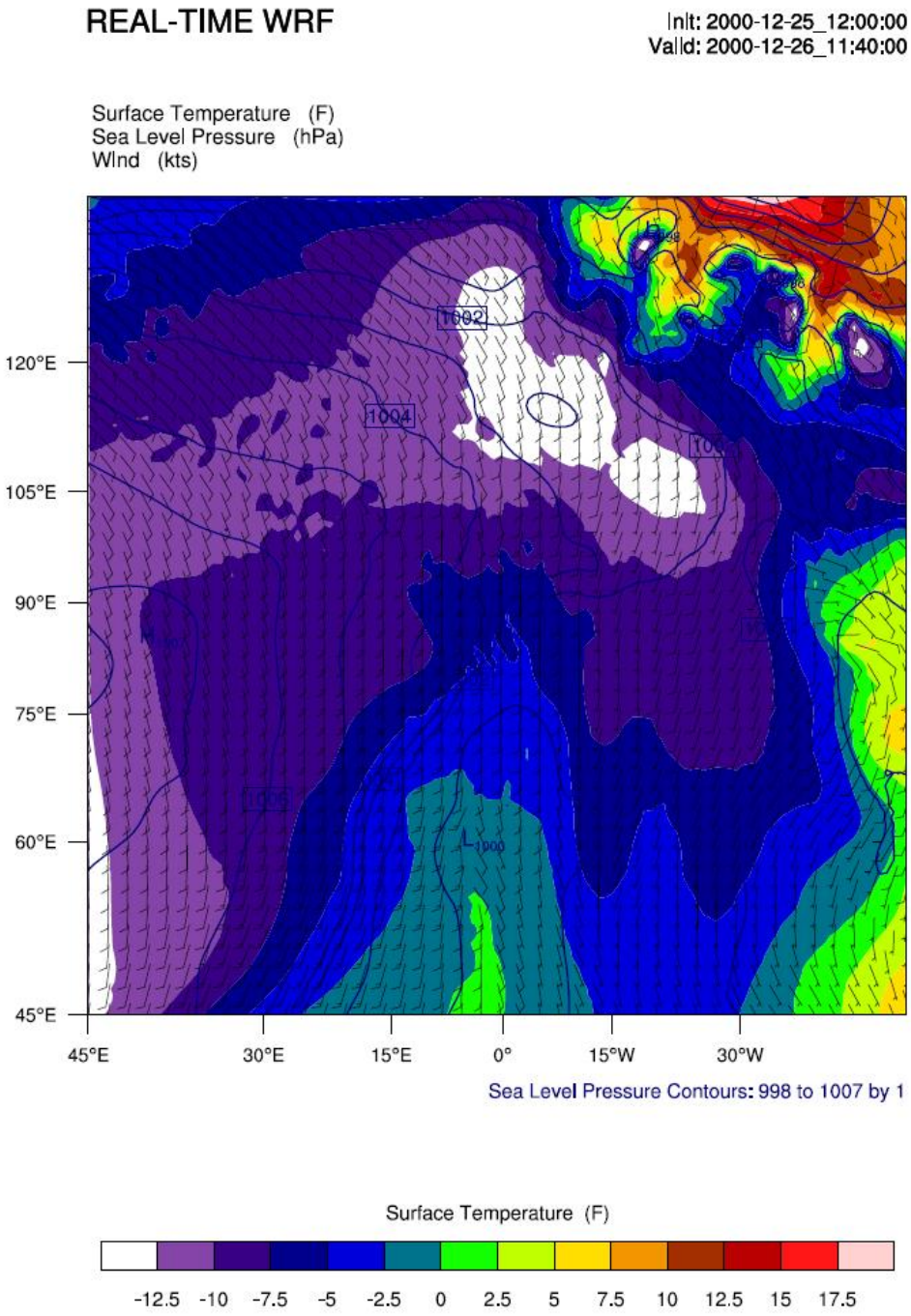

Figure 7.4a: AMPS WRF output for Case 2, depicting surface pressure, temperature, and winds (*image: Suraj Harshan)*

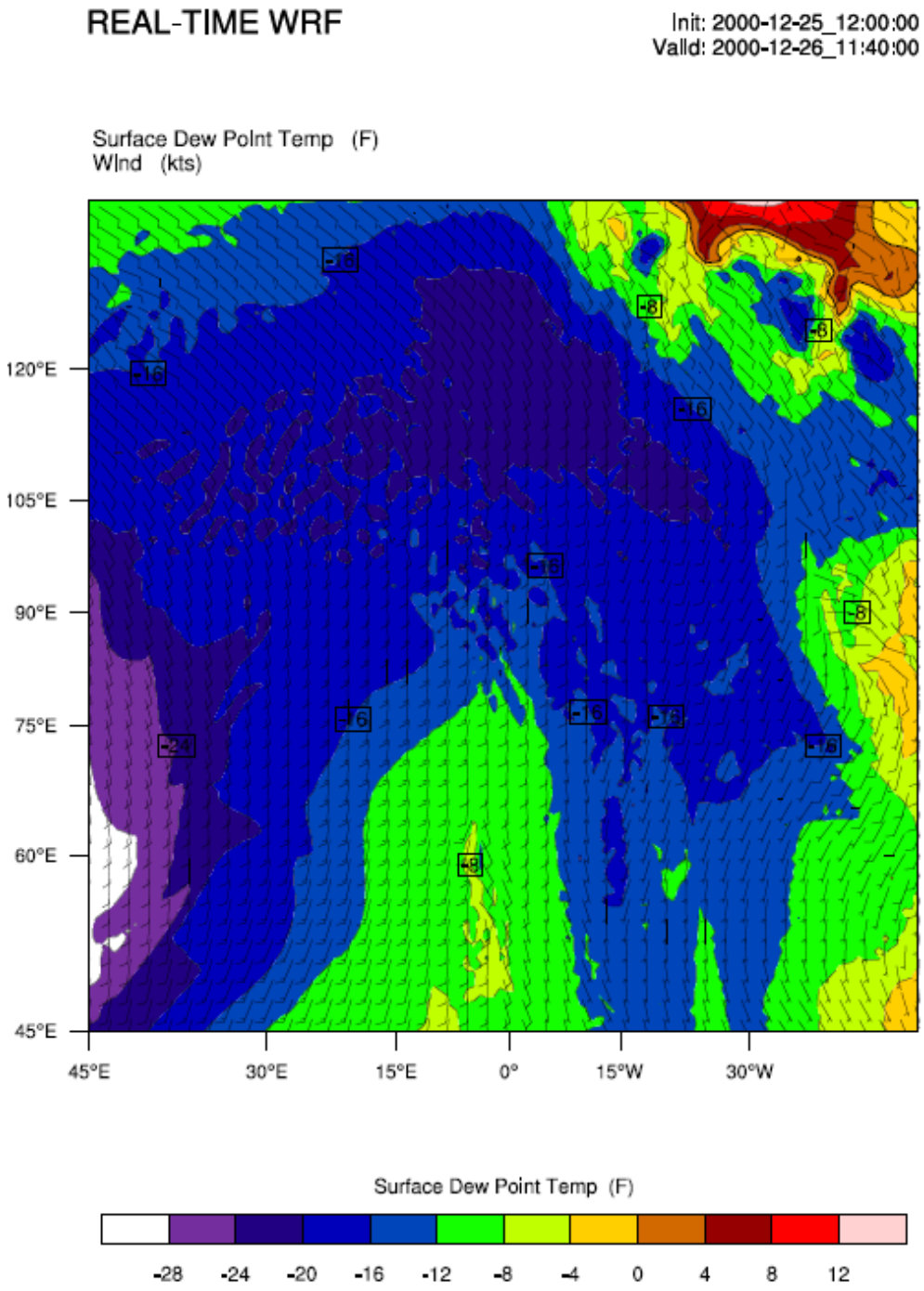

Figure 7.4b: AMPS WRF output for Case 2, depicting surface pressure, temperature, and winds (*image: Suraj Harshan)*

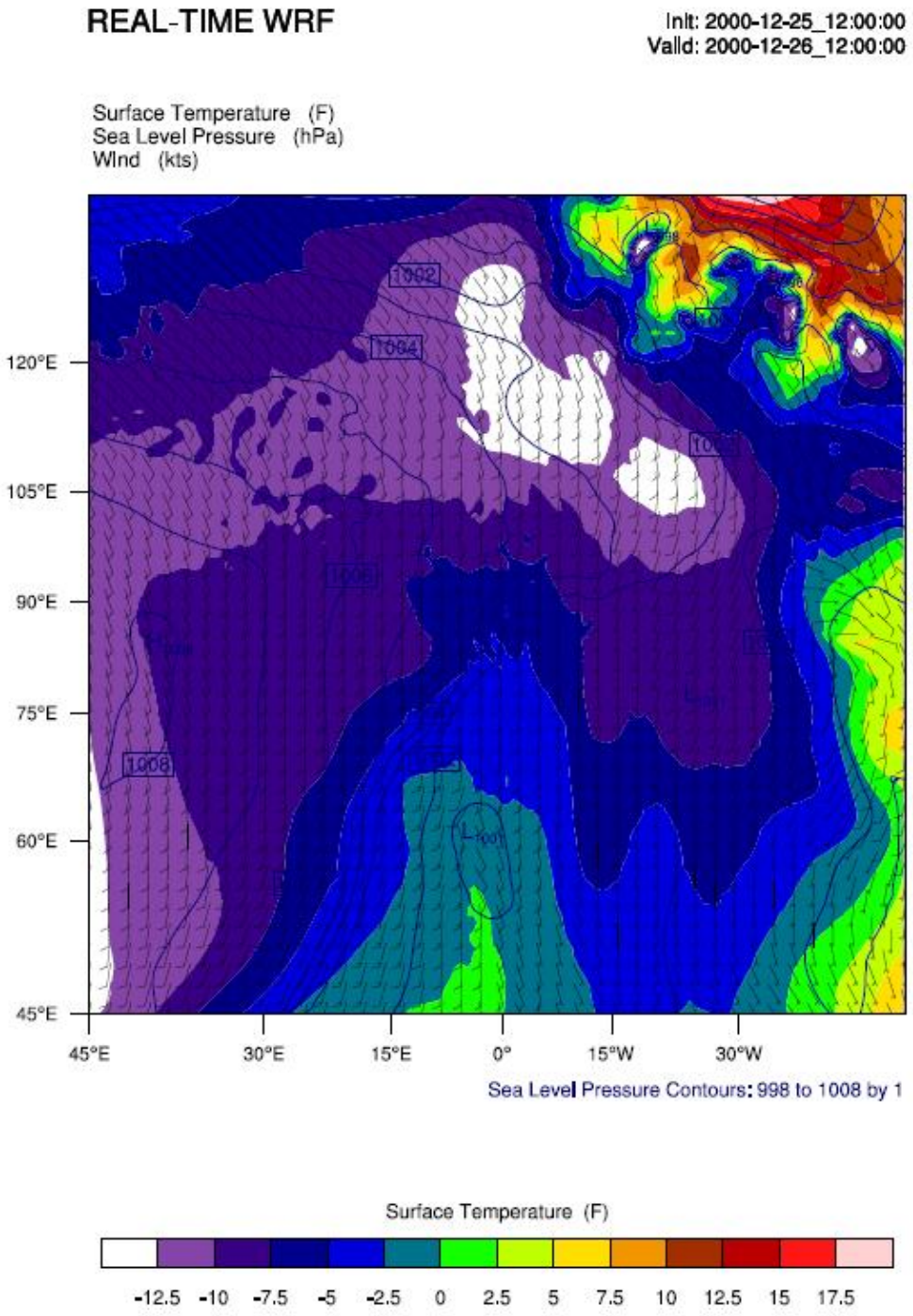

Figure 7.4c: AMPS WRF output for Case 2, depicting surface pressure, temperature, and winds (*image: Suraj Harshan)*

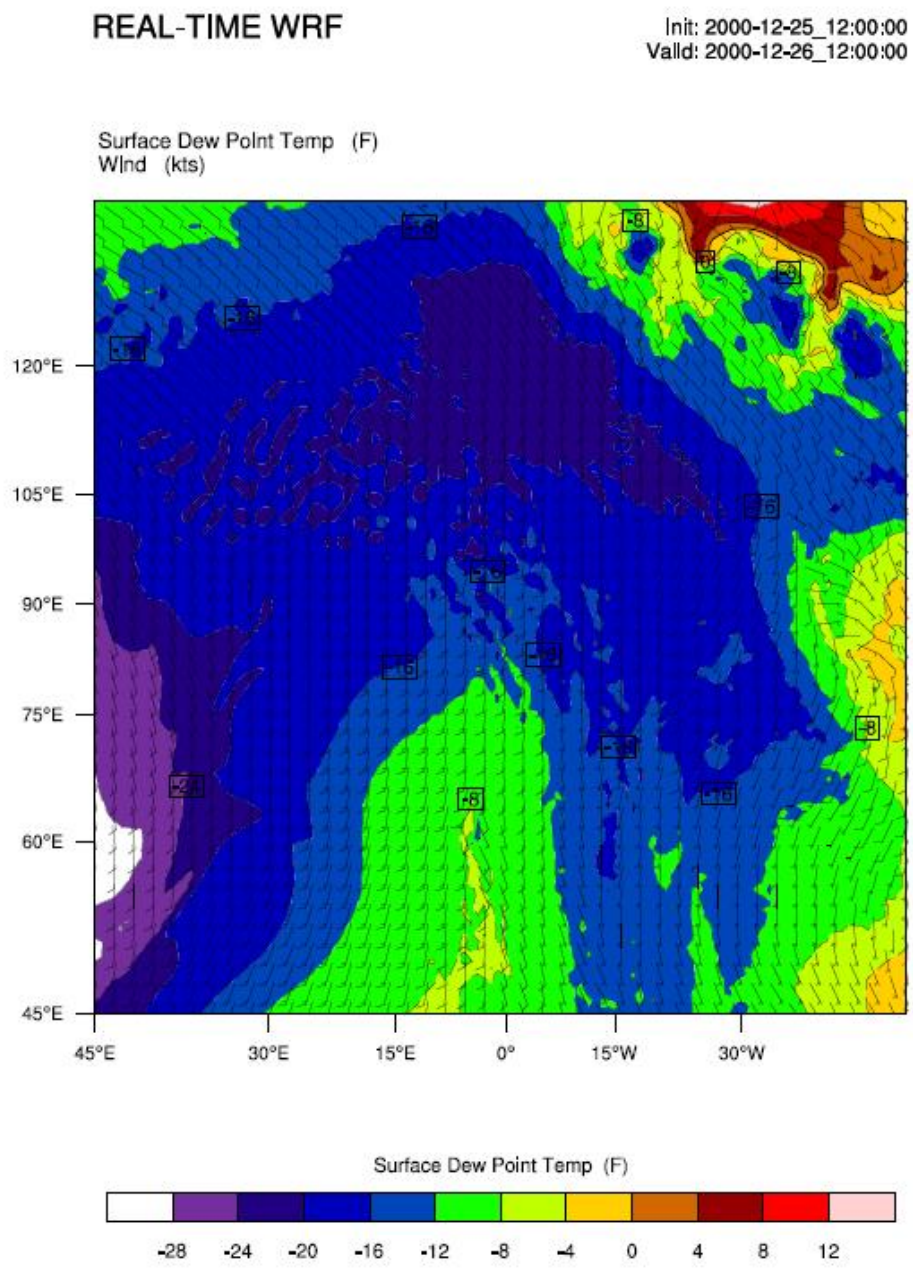

Figure 7.4d: AMPS WRF output for Case 2, depicting surface pressure, temperature, and winds (*image: Suraj Harshan)*

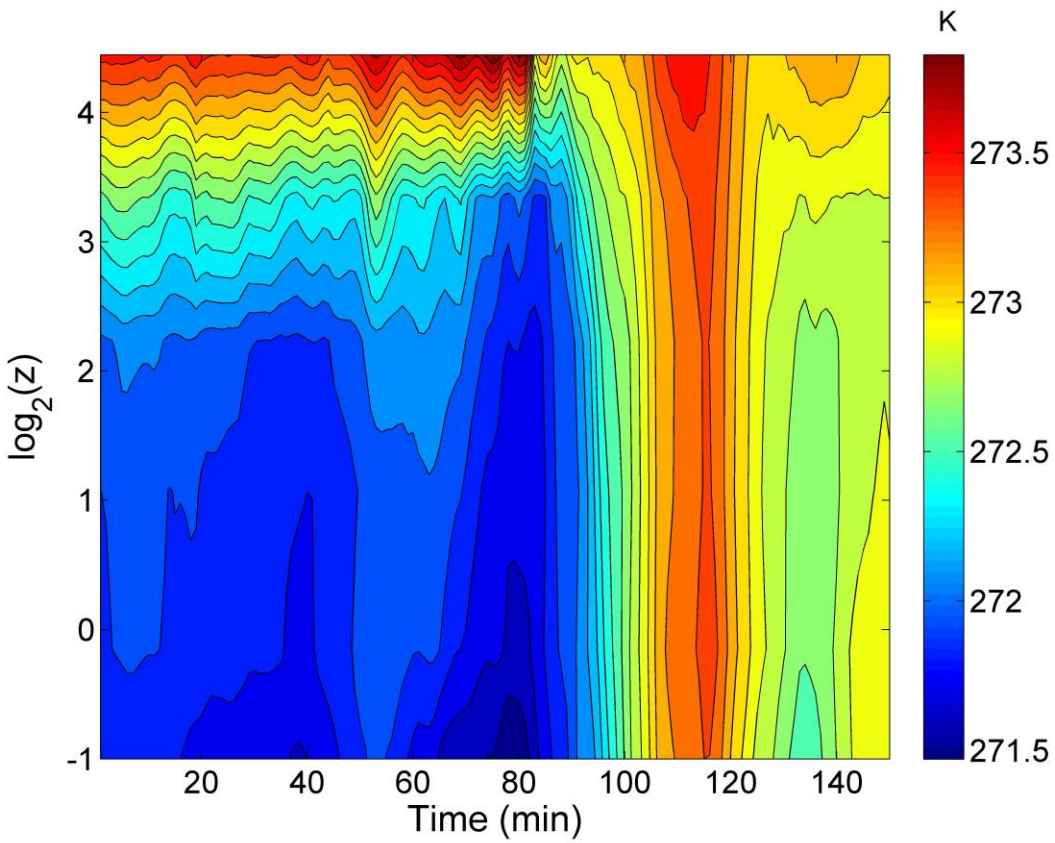

Figure 7.5: Time-height plot of potential temperature for Case 1

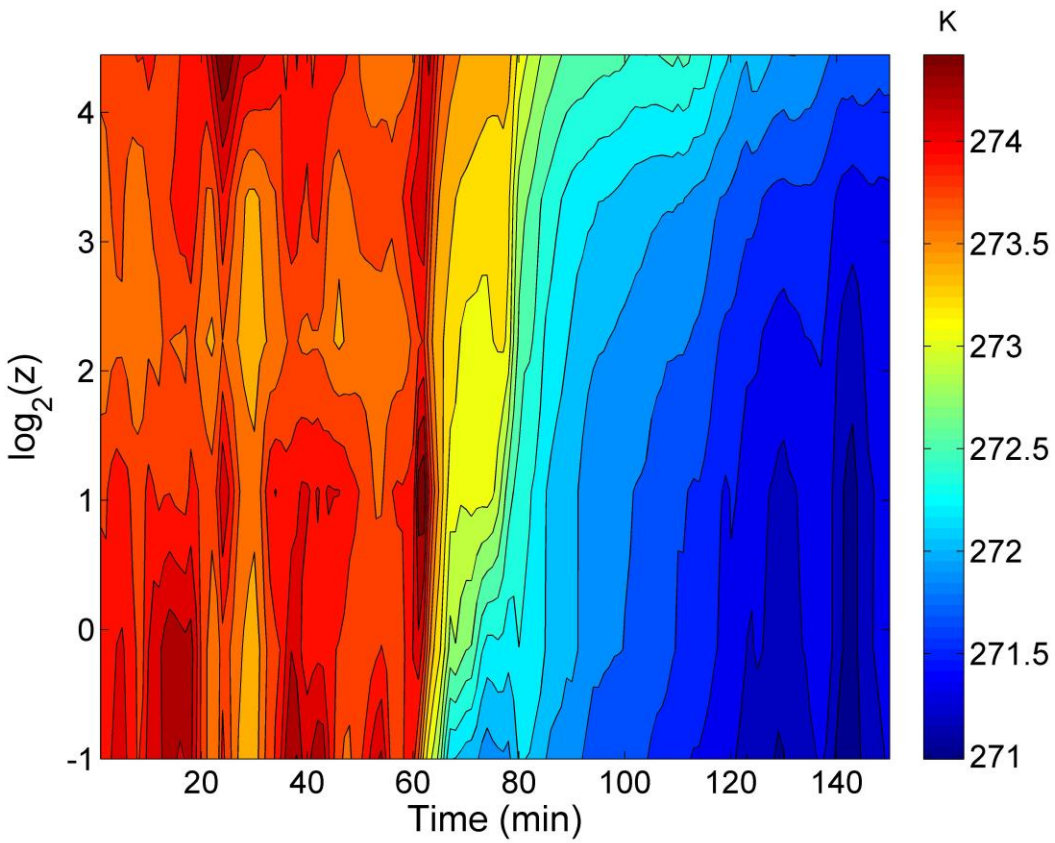

Figure 7.6: Time-height plot of potential temperature for Case 2

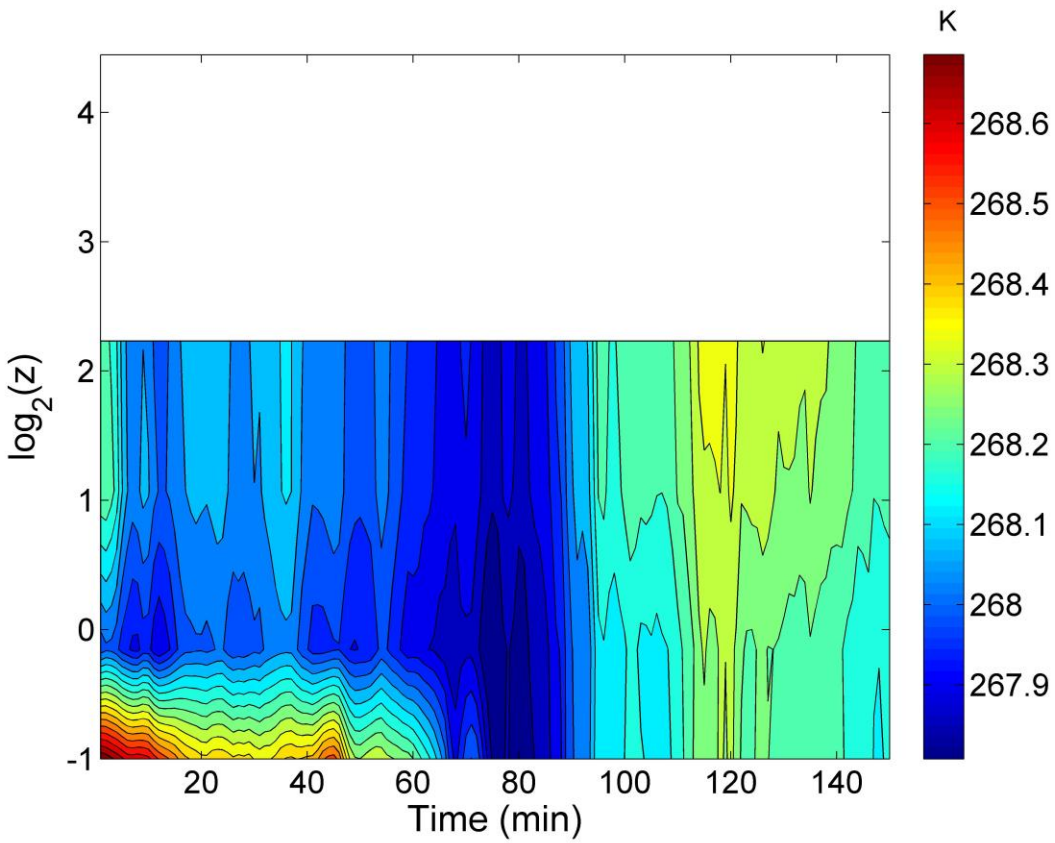

Figure 7.7: Time-height plot of potential temperature for Case 3 (*note: data missing at upper levels due to malfunction of sensors)*

Table 7.1

Parameter		3.1m Anemometer	7.0m Anemometer
CASE 1:	L	14.05	5.16
	z/L	0.22	1.36
	u_*	0.04	0.04
CASE 2:	L	12.92	7.01
	z/L	0.23	1.00
	u_*	0.07	0.05
CASE 3:	L	10.20	4.01
	z/L	0.30	1.75
	u_*	0.07	0.05

Values computed for M-O length (L), the ratio of height to M-O length (z/L), and friction velocity (u_*) from data collected during Cases 1, 2, and 3.

CHAPTER 8

TURBULENCE SPECTRA

8.1 Turbulence Spectra in the Antarctic Boundary Layer

A method that will provide a new perspective as to the role of turbulence in the stable boundary layer is converting scales of motion to their spectral representations, thereby associating the amounts of variance, energy fluxes, and kinetic energy to each spectral range (the energy-containing range, inertial subrange, and dissipation range), allowing for a better idea of overall boundary layer structure (Kaimal et al., 1993). It is important when examining the stable boundary layer, to discern between the larger "energy-containing" eddies, which can be attributed to gravity waves or the passage of synoptic-scale weather systems and the smaller eddies resulting from the breakdown of these large-scale eddies, and subsequent energy transport to smaller and smaller scales that result in bursts of turbulence.

In boundary layer flow, there are three major spectral regions, as identified before: the energy-containing range, the inertial subrange, and the dissipation range. As described by Kaimal et al. (1993), the energy-containing range contains most of the turbulent energy, and in this range, the energy is produced by both buoyancy and shear. Conversely, in the dissipation range, we find the smallest scale fluctuations, where kinetic energy undergoes a conversion to internal energy. Between these two ranges, the inertial subrange serves as a

transition zone. In this range, energy is not produced, nor is it dissipated, and therefore, the range allows for the migration of the large eddies of the energy-containing range to transition to the smallest eddies of the dissipation range. Also, in the inertial subrange, turbulence can be assumed to be isotropic, which simply means that the velocity field is independent of any reflection or rotation about the spatial axes (Kaimal, 1993). Stull (1988) elaborates upon this idea further; stating that the middle size turbulent eddies found in the inertial subrange feel neither the effects of viscous forces nor the generation of turbulence kinetic energy. Essentially, it is in this range that energy 'cascades' from the largest scales to the smallest. In the inertial range, there are only three variables relevant to flow: **S** (spectral energy density), **κ** (wavenumber), and **ε** (turbulence kinetic energy dissipation rate). It is important to note that in this range, the transfer of energy is controlled entirely by **ε**.

8.2 An Overview of Turbulence Spectra

The role of turbulence in the stable boundary layer is different than that in the mixed layer or convective boundary layer, and these differences are important to note when studying the spectra of these layers. In the stable layer, the variances and covariances of the wind velocity and temperature obey local similarity theory and local scaling. Furthermore, the variance of velocity fluctuations (u') has the same units as turbulence kinetic energy per unit mass, and it is the u component of the velocity which will be the main focus of this

thesis. Also, as presented by Kolmogorov (1941), using dimensional analysis, it can be shown that one-dimensional velocity spectra strictly follow a -5/3 power law in the inertial subrange. However, in order to perform a spectral analysis of a dataset, the mathematical background of spectral analysis and related fast Fourier transforms must be examined, and assumptions used in these calculations should be highlighted (see Appendix A for further information regarding the Fast Fourier Transform).

8.3 Characteristics of the Inertial Subrange

As was discussed previously, the -5/3 power law is a very important indicator of the inertial subrange of turbulence in the stable boundary layer. It is in this range that energy is neither created nor destroyed, and therefore the cascade rate of energy through the turbulent spectrum is required to equal the rate of dissipation at the smallest scales.

Stull (1988) in turn provides a simple proof applying Buckingham Π analysis, creating a dimensionless group from the variables in section 8.1 in equation 8.3.1.

$$\pi_1 = \frac{S^3 \kappa^5}{\varepsilon^2} \tag{8.3.1}$$

And, it can be assumed that this equation is equal to a constant, and therby, solving for S yields 8.3.2, where the -5/3 exponent over **κ** dictates the dissipation rate of turbulence through the scales, and therefore, the transfer rate through the inertial subrange.

$$S(\kappa) = \alpha_k \varepsilon^{2/3} \kappa^{-5/3} \tag{8.3.2}$$

8.4 Characteristics of Antarctic Data

The boundary layer over the Antarctic continent is strongly stratified. While analyzing Antarctic observations, previously Humi (2002) reported the existence of an additional range of turbulence, beyond the energy containing range, inertial subrange, and dissipation range. Due to the strong stratification of the Antarctic boundary layer where lapse rates can occasionally approach 1K/m, Humi (2002) contemplated the existence of buoyancy range turbulence (hereafter, BRT) which would flatten the spectra of the time series in parts of the inertial range. Humi (2002) continues to explain that in analyzing Antarctic data, there was found to be a -3 slope in part of the inertial range, and literature on the subject considers this to be a strong indicator of 2-d turbulence (Figure 8.1). Upon analyzing ISCAT-00 data using spectral analysis, the existence of BRT will be explored as will general spectral characteristics of the datasets. This will, in turn, allow for comparison to Humi (2002), to find any similarities or differences that may exist.

8.5 Spectral Analysis Results

Upon the analysis of the data in Cases 1, 2, and 3 from the ISCAT-00 campaign, it was clear that the -5/3 power law relationship as described previously was satisfied. Figures 8.2, 8.3, and 8.4 display the spectra for Case 1,

Case 2, and Case 3 respectively, with the 3.1m longitudinal velocity spectra plotted in red, 7.0m longitudinal velocity plotted in blue. At both levels, the -5/3 power law was obeyed over nearly all frequencies.

Upon comparing these findings with those of Humi (2002), several important factors can be noted. First, Humi (2002) described the area with -3 slope as being a part of the BRT spectrum, and this slope was not indicated in the three data sets that were analyzed from ISCAT00. Despite this, the presence of BRT cannot be disproved, because ISCAT00 data was collected during the Antarctic summer, when the boundary layer was not as strongly stratified as it was during the data collection for Humi's (2002) observations in June. Therefore, it can be hypothesized that if the data were to have been collected during the Antarctic winter, trends similar to those found by Humi (2002) might be observed.

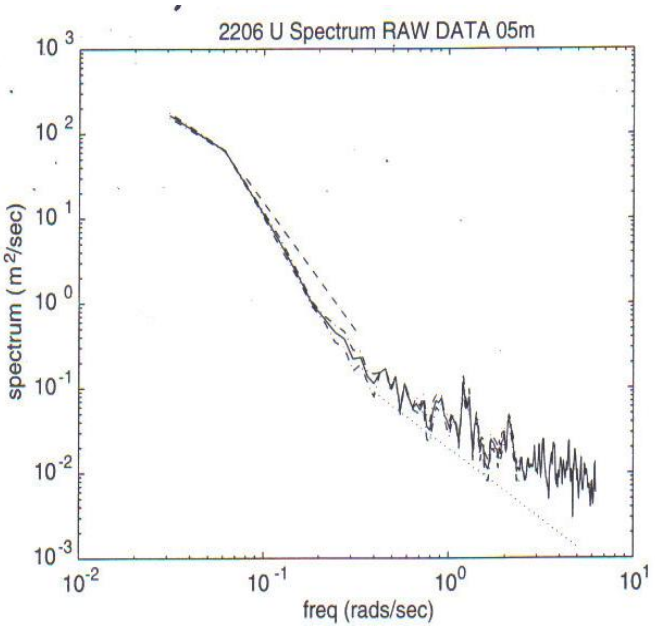

Figure 8.1: Spectra of the raw data of U at 5m height, the dotted line representing that of the -5/3 slope, and dashed representing that of the -3 slope, indicating the presence of BRT (*image: Humi, 2002)*

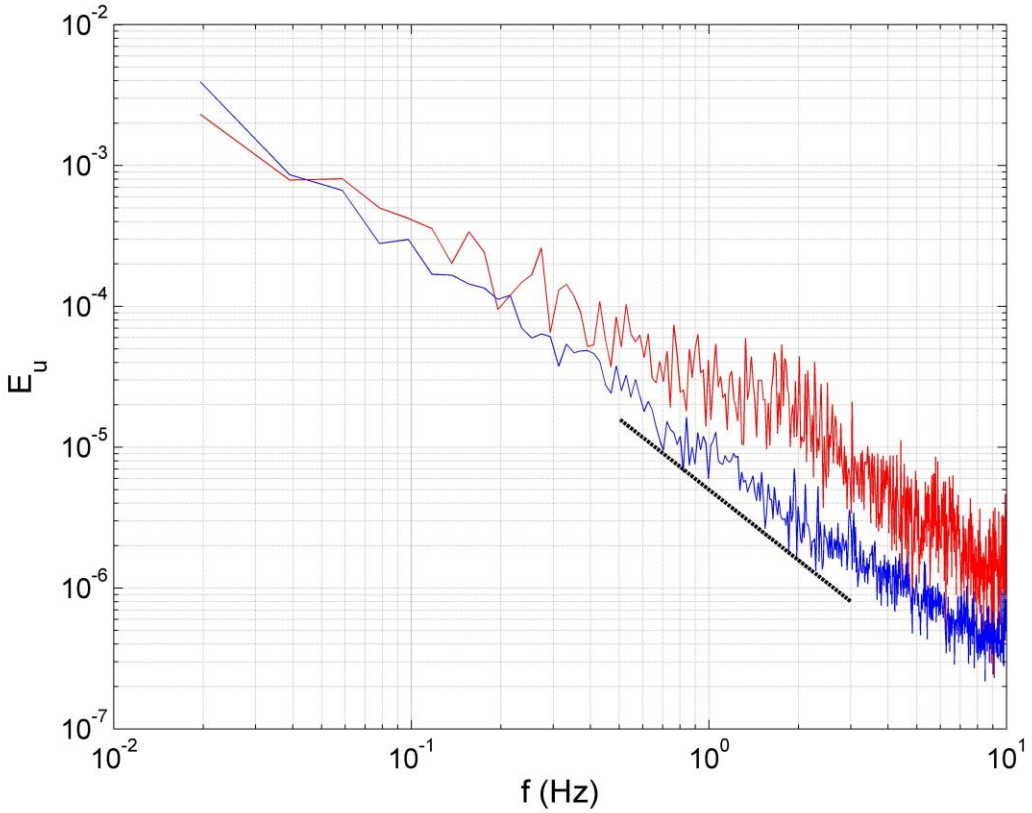

Figure 8.2: Spectra of the data of U at 3.1m (red) and 7.0m (blue), the heavy line representing the -5/3 slope (Case 1).

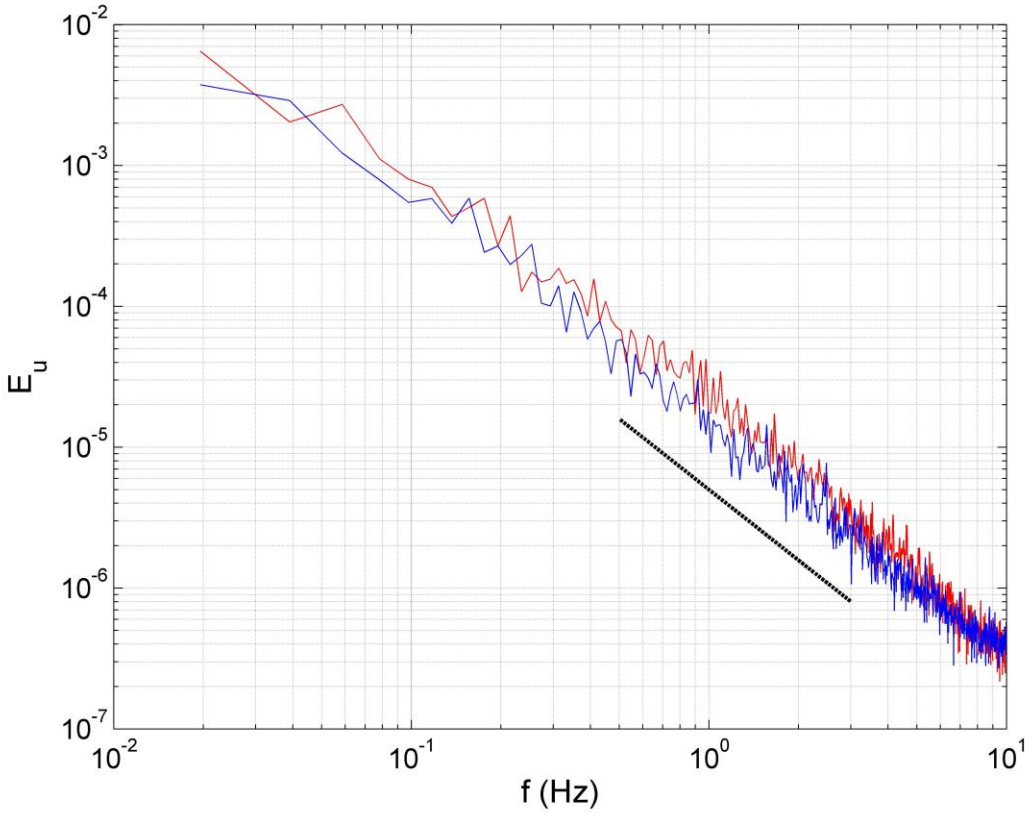

Figure 8.3: Spectra of the data of U at 3.1m (red) and 7.0m (blue), the heavy line representing the -5/3 slope (Case 2).

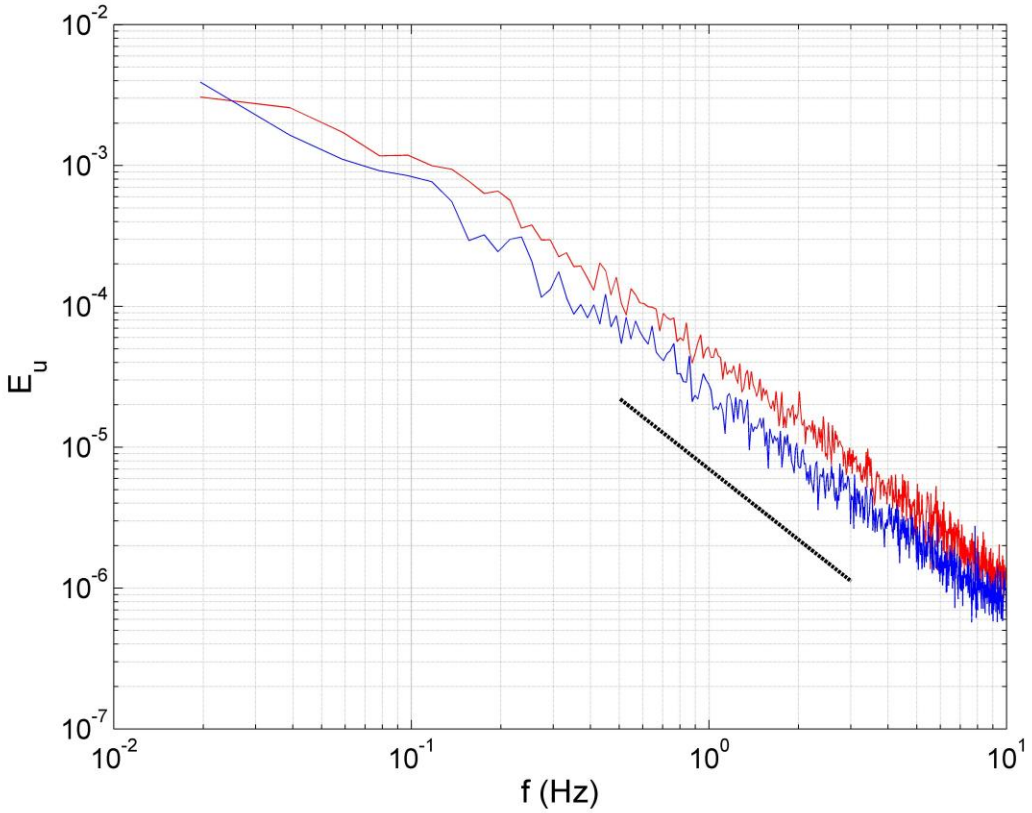

Figure 8.4: Spectra of the data of U at 3.1m (red) and 7.0m (blue), the heavy line representing the -5/3 slope (Case 3).

CHAPTER 9

ADAPTIVE COHERENT STRUCTURE DETECTION METHODOLOGY

9.1 Development of an Adaptive Coherent Structure Detection Technique

In developing a new coherent structure detection methodology, the first step was to build upon a pre-existing method, chosen to be that of Nakamura and Mahrt (2005). As was discussed in Chapter 5, the primary drawbacks of this methodology were the threshold and window size, both which were highly subjective, and depending on the window size used and the threshold value selected, the number of events detected at both 3.1m and 7.0m on the ISCAT-00 tower significantly increased (with decreasing threshold and window size) and decreased (with increasing threshold and window size). So, the primary goal of the new methodology is to remove the subjective nature of the Nakamura and Mahrt (2005) method, allowing for the creation of a newer, more robust means of identifying the onset of turbulent bursting and the characteristics of corresponding coherent structures.

The idea of using an adaptive threshold was adopted for the newly developed method, which would allow for the characteristics of each individual data set to dictate a threshold most suitable for the data at hand. An adaptive threshold would serve to remove a large portion of the subjectivity in the pre-existing Nakamura and Mahrt (2005) method, and is felt that it would provide a better, truer idea of the properties of atmospheric turbulence contained within a

series. First, the chosen data set would undergo a surrogate analysis. This analysis would serve to test the hypothesis regarding whether the bursting events can be explained by linear stochastic processes, or if there is any nonlinear phase correlation involved. The benefits of using a surrogate analysis were simply that since the surrogate series was nothing more than the data points in the original series organized into a random fashion, that the surrogate would maintain the probability distribution function, autocorrelation, and spectra found to be associated with the original data set. Once the surrogate is obtained from a set identified as being turbulent by the Nakamura and Mahrt (2005) method, the method is once again applied to the surrogate, and if the set does not qualify as having any coherent structures, it is proven that the turbulent bursting found to have occurred is a non-linear phenomena, and can therefore not be explained by simple linear stochastic processes.

For the adaptive threshold method, it was decided to use 100 different surrogates from the same 'parent' data set and in turn, apply the Nakamura and Mahrt methodology to each surrogate set, in order to discover whether events were indicated. Since each surrogate set was proven to be linear, and since the points were re-ordered in a random fashion, no specific threshold would be chosen. The sets would simply be analyzed, and the maximum TEI value for each surrogate set, given the Nakamura and Mahrt method, would be recorded, and archived for the next step in the adaptive threshold method. Once all 100 sets were analyzed, the maximum TEI for each set would be ordered in

descending value, from the highest recorded TEI to the lowest. Then, this set of TEI values for the surrogate sets would be ordered from maximum to minimum, and using a significance level (alpha, α) of 0.1, an adaptive TEI threshold would be selected. It is felt that the threshold value identified closest to this value, yet within the confidence interval, would serve as the critical threshold of the data set. So, essentially, the threshold identified would be that which is most unique to the original turbulence data set, and also that which would serve to better identify non-linear turbulent bursting events. Once the threshold was in place, the Nakamura and Mahrt methodology would be executed once more, and findings using the new adaptive threshold would be recorded, which is discussed in further depth in the following section.

Important to note, however, is though this method only directly addresses the subjective threshold problem, the problem associated with window size is indirectly addressed. When considering the ideal window size, a relationship between window size and threshold is forged, since the threshold found using the technique would automatically adjust as window size increased or decreased (as the the window size grows smaller, the threshold would increase). Despite this, there is still no concrete method for dictating window size, though the data proves that the window size should be small enough to detect the smaller, shorter-lived bursting events, but also should be large enough for a reliable computation of standard deviation within the window. The 5 minute time interval dictated by Nakamura and Mahrt (2005) was not utilized here, nor was it included

in the adaptive methodology, simply because there is no way to be sure without a concrete definition of coherent structures, whether 5 minutes is truly long enough to capture an entire burst, or if it is far too long. The method itself is simply a new, robust way to identify turbulent bursting events and corresponding coherent structures using the properties of the series at hand to the advantage of the researcher to paint a clearer picture of the behavior of stable boundary layer turbulence by removing subjectivity from the analysis, allowing for more reliable analysis results.

9.2 Adaptive Methodology Results

After conducting the analysis using the adaptive threshold method, drastically different results were found for the same data set than when the Nakamura and Mahrt technique was used. Using the significance level of $\alpha = 0.1$, it was found that given the data set and its unique characteristics, that the threshold of 3 employed by Nakamura and Mahrt (2005) was far too large in all three of the cases. Figures 9.1, 9.2, and 9.3 depict the adaptive results from Case 1, Case 2, and Case 3 respectively, and again, the red plots correspond to sonic anemometer data collected at 3.1m, and the blue plots correspond to 7.0m data.

Case 1 contained 2 onsets of bursting at each level, as identified by the adaptive threshold technique. At 3.1m, the onset of the first event was identified around 11 minutes into the time series, and the first event at 7.0m was identified

at near 13 minutes. This could possibly indicate that the turbulent burst identified using this technique could have begun due to instability at lower levels which then propagated upward. The second onset of bursting identified occurred at both 3.1m and 7.0m at 25 minutes, possibly indicating a fairly large vertical extent of the turbulent patch. Using this time series, the adaptive threshold technique needed to identify the onset of bursting events at 3.1m was only ~1.4, and at 7.0m, ~2.2, both of which are significantly less than the Nakamura and Mahrt threshold of 3.

Upon analyzing Case 2 using the adaptive threshold methodology, 2 onsets of bursting were identified at 3.1m, and 3 onsets were identified at 7.0m. Again as in Case 1, there were onsets indicated simultaneously at both levels. In this data set, this occurred around 13 minutes, and 17 minutes, as shown in Figure 9.2. A third event, indicated only at 7.0m began at around 21 minutes. The thresholds identified using the adaptive method in this case were also significantly less than the Nakamura and Mahrt threshold of 3, at only around 1.5 at both levels.

Finally, Case 3 contained the most onsets of bursting as indicated by the new method, with 4 at both levels on the tower. Given the times of onset, it appears that the first two events identified at each level could have possibly been to instability propagating upward as described in the Case 1 discussion. The first event was recognized at 5 minutes at 3.1m, and 6 minutes at 7.0m. The second onset was shown to occur at 12 minutes at 3.1m, and 14 minutes at 7.0m. The

third and fourth events were indicated at both levels at the same time, at 18 minutes and 25 minutes, respectively. Also, once again, the thresholds were much smaller than the constant threshold of 3 as put forth by Nakamura and Mahrt. At 3.1m, the threshold needed to identify bursting was only around 0.8, and at 7.0m, 1.9.

Given the results found by using the adaptive threshold method, it can be discerned that the threshold of 3 that Nakamura and Mahrt suggest could be far too large to correctly identify onsets of bursting in the stable boundary layer. With a larger threshold, it is possible to miss smaller events, that given their respective time series, are events of significance. Also, the Nakamura and Mahrt method employs the use of a 5 minute average to compute the TEI of the time series, which could result in unintentional smoothing of the dataset, thereby losing characteristics of smaller bursting events. The one minute time average used by the adaptive technique serves to alleviate this problem. One final subjective problem addressed with the adaptive method was the idea that no event onsets would be identified within 5 minutes of a previously defined onset, as described by Nakamura and Mahrt (2004). Since there is currently no concrete definition of what a coherent structure is, it is unknown whether 5 minutes is either adequate enough to encompass the entire life cycle of a burst, or if it is not long enough to allow for the generation and dissipation of a coherent structure; so this criteria was not employed. All of the events identified using the new technique would satisfy this criteria, however, in Case 2, the second event at

both levels would not have been identified, since it occurs only 4 minutes after the previous onset (Figure 9.2). Also, in Case 3, the third defined onset at 7.0m would not have been considered, since it too occurs only 4 minutes after the previous 7.0m onset (Figure 9.3). It is felt that the adaptive threshold technique is more accurate in this sense, due to the use of the surrogate of the original data set, which allows for the preservation of the probability distribution function, autocorrelation, and spectral characteristics of the time series.

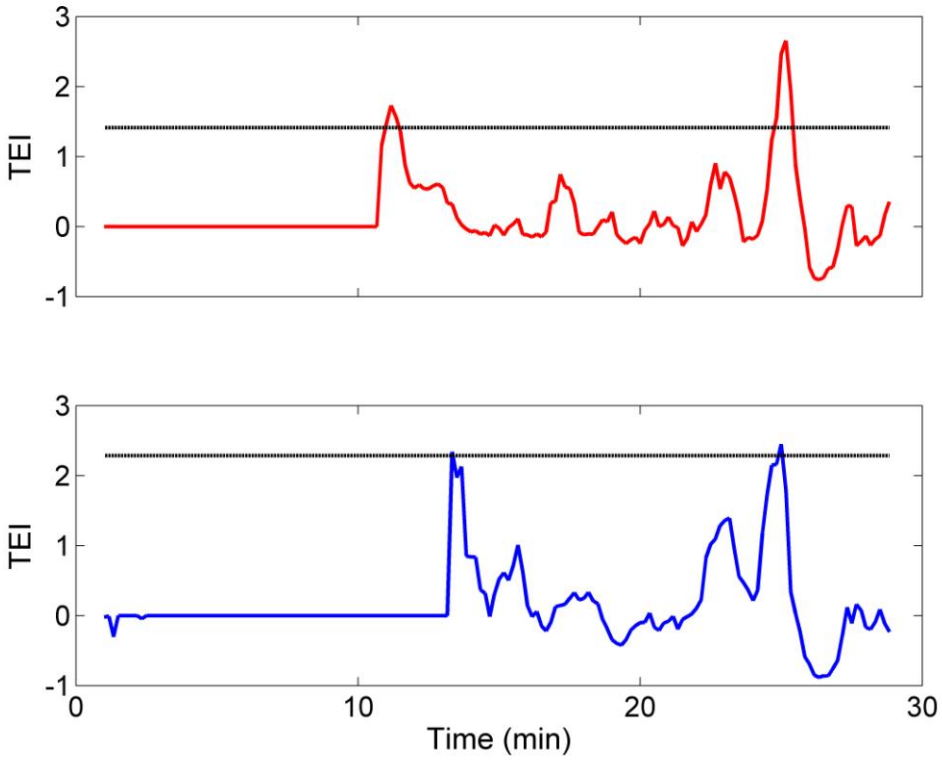

Figure 9.1: Adaptive threshold results for Case 1, red line indicates TEI values for 3.1m data, and blue indicates TEI values at 7.0m. The black line in each case shows the adaptive TEI threshold, as found as using the new methodology.

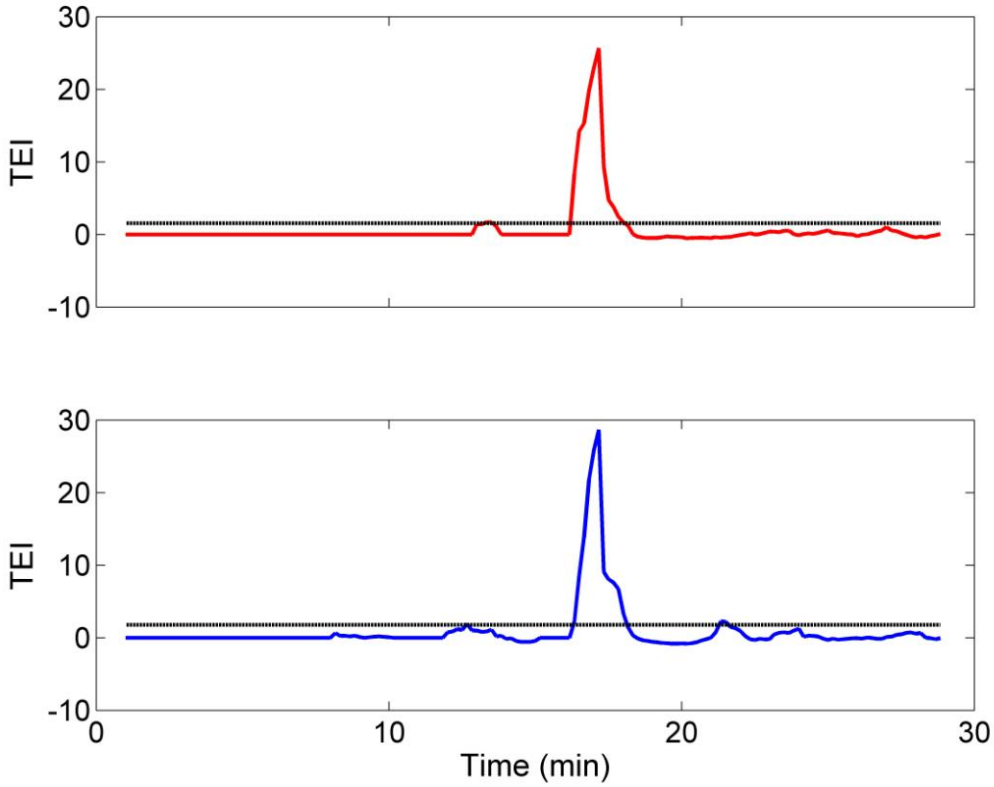

Figure 9.2: Adaptive threshold method results for Case 2, same conventions as in Figure 9.1.

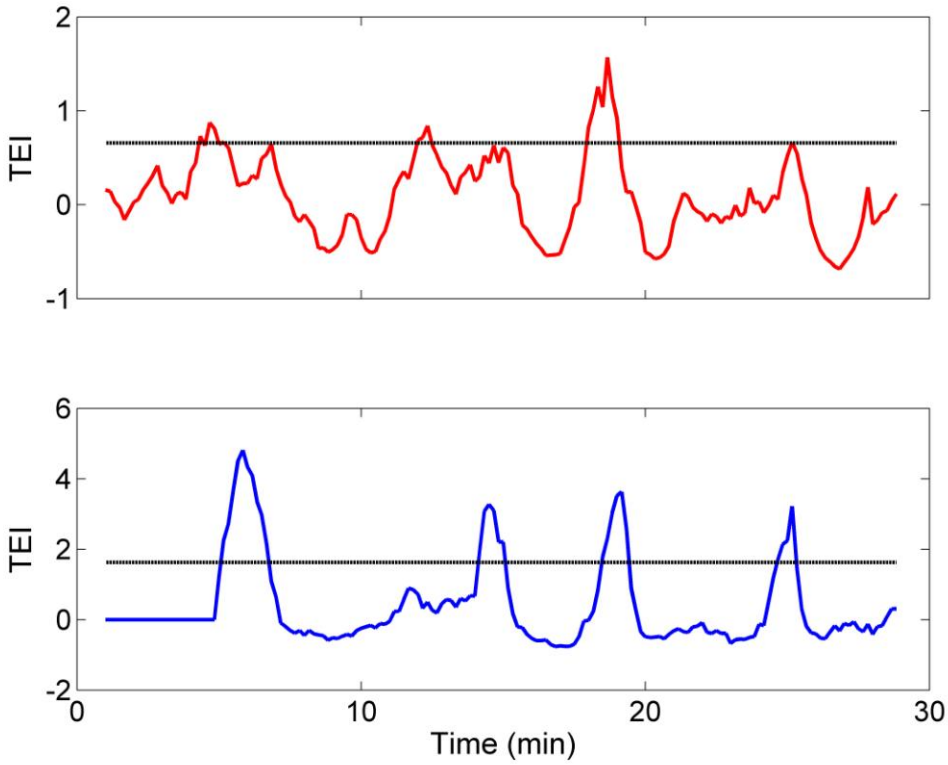

Figure 9.3: Adaptive threshold method results for Case 3, same conventions as in Figure 9.1.

CHAPTER 10

SUMMARY AND DISCUSSION

10.1 Summary

Of nearly all the boundary layer modeling parameterizations, the parameterizations that cause the most problems concern the stable boundary layer and flux transfers near the surface. Before these parameterization problems can be rectified, the scientific community as a whole must have a better understanding of the properties of the stable boundary layer. Bursting events that occur during otherwise stable conditions have been a continued problem for researchers, nobody really able to cohesively define what a coherent structure is, and only speculation as to their cause.

Using data collected during the ISCAT-00 campaign, methods of identifying and studying turbulence bursting events in the stable layer were able to be employed in a region previously unexplored in such a way. A large number of studies had been done regarding turbulent bursting episodes during the CASES-99 experiment, allowing for the development for methodologies that proved useful in a transitionally stable boundary layer. These methods could then be applied to a more persistently stable regime, not only to test the validity of said methods, but to also further understand the atmospheric conditions at hand.

In this research, a new adaptive threshold technique was created, building upon a coherent structure detection method as described by Nakamura and Mahrt (2005) in order to take a more robust approach in identifying bursting events. It proved to be very successful, accounting for many of the subjective loop-holes in the original methodology. The adaptive technique takes a unique approach in allowing the data set itself dictate the relevant threshold for coherent structure detection, and prevents the loss of detail when exploring a data set for turbulent bursting events. When compared side by side, the adaptive threshold technique proved to be more reliable than the previous coherent structure detection method, though there are still opportunities to test it over a wider range of environments, to see if it remains a viable way to explore the characteristics of the stable boundary layer.

In addition to the development of the new method, a spectral analysis of turbulence in the Antarctic boundary layer was performed, and compared to previous studies, and also compared to the characteristics of turbulence spectra in mid-latitudes. It was found that the turbulence spectra in the persistently stable boundary layer closely resembled that found in the transitionally stable boundary layer, though there is still much opportunity to explore this further, especially when it comes to proving or disproving the existence of Buoyancy Range Turbulence, as described by Humi (2002).

So, at this time, it would be deemed appropriate to revisit the questions posed in Chapter 1, that were hoped to be answered by this research.

1. Do turbulent bursting events and corresponding coherent structure exist in the Antarctic?
2. Can any causes of bursting in the stable layer be easily identified?
3. How does local stability play a role?
4. Can spectra analysis discern turbulent bursting events?
5. Is it possible to determine an objective technique for coherent structure detection?

In addressing question 1, using both the coherent structure detection methodology and the new adaptive threshold detection methodology, it can be answered with confidence that yes, turbulent bursting events do exist in the Antarctic. Yet, the duration of these events is still questionable. Through this research, model data was used in order to possibly identify a meteorological cause or triggering mechanism for turbulent bursting events, and there were several small scale possibilities found that could result in the onset of an event. However, there were never any large scale meteorological phenomenon that were observed in conjunction with the onset of the bursts described in the three cases studied. So, the answer to question 2 is no, there are no easily identifiable concrete causes of the turbulence that occurred during ISCAT-00. Regarding question 3, about local stability, it was found that the events occurred during a less stable period, which could simply be due to the fact that during ISCAT-00, it was the Antarctic summer. There is also no definitive answer whether bursting can only be classified as occurring during extremely stable periods versus less

stable. Therefore, the answer to question 3 is a bit ambiguous yes and no. One key feature analyzed in this research was that of the spectra of the three time series during which turbulent bursting onsets were defined. Upon analyzing the spectra, it was found that it closely followed the -5/3 power law as described by Kolmogorov (1941). This indicates that, due to the lack of any irregularities in any of the three cases, that no, turbulent bursting in this case could not be discerned by simple spectral analysis, and was therefore nonlinear. Finally, question 5 regards the possibility of developing an objective technique for turbulent bursting event detection and identification. The answer to question 5 is that yes, this is possible, and the new adaptive threshold technique is an example of this.

10.2 Future Direction

There are several ways this research could be further expanded on in the future. First, it would be beneficial to apply the new adaptive threshold technique to data collected in midlatitudes, perhaps from the CASES-99 experiment. Also, if at all possible, it would be interesting if any data from the Arctic could be obtained, in order to compare turbulence characteristics between the two Polar regions. Furthermore, it would be beneficial to discern more regarding the spectral characteristics, especially to determine the existence of BRT, to back up previous findings, and to figure out that if it does exist, whether it us confined primarily to the poles, or if it can be observed in other regions around the globe.

One final future possibility for this research is a possible 'reversal' of the adaptive threshold technique, which would enable the detection of the dissipation portion of a bursting event. If this were to occur, it could be coupled with the onset detection method, and thereby be used to discern the approximate lifespan of the observed turbulent bursts, something that has yet to be accomplished in the field.

This leads to the ultimate goal for this research, and any completed afterward, which is that advances are made toward fully understanding the characteristics of turbulence in the stable boundary layer, and what causes it, and possibly how to forecast it. If this were to be accomplished, it would have extensive positive repercussions not only in the meteorological field, but also the field of air pollution modeling, and renewable energy endeavors. It is certainly something that must be further studied, to increase understanding, and to apply to modeling efforts overall, not only to increase the accuracy of stable boundary layer modeling, but to better model the surface layer as a whole.

REFERENCES

Banta, R., Y.L. Pichugina, and R.K. Newsom, 2003: Relationship between low-level jet properties and turbulence kinetic energy in the nocturnal stable boundary layer. *J. of Atmo. Sci.* **60,** 2549-2555.

Basu, S., F. Porté-Agel, E.F. Foufoula-Georgiou, J-F Vinuesa, and M. Pahlow, 2006: Revisiting the local scaling hypothesis in stably stratified atmospheric boundary-layer turbulence: An integration of field and laboratory measurements with large eddy simulations. *Boundary-Layer Meteorol.* **119,** 473-500.

Blackwelder, R.A., and R.E. Kaplan, 1976: On the wall structure of the turbulent boundary layer. *J. Fluid Mech.* **76,** 89-112.

Cassano, J.J, T.R. Parish, and J.C. King, 2000: Evolution of turbulent surface flux parameterizations for the stable surface layer of Halley, Antarctica. *Mon. Wea. Rev.* **129,** 26-46.

Chimonas, G., 1998: Steps, waves, and turbulence in the stably stratified | planetary boundary layer. *Boundary-Layer Meteorol.* **90,** 397-421.

Coulter, R.L, and J.C. Doran, 2002: Spatial and temporal occurrences of intermittent turbulence during CASES-99. *Boundary-Layer Meteorol.* **105,** 329-349.

Dabberdt, W.F., D.H. Lenschow, T.W. Horse, P.R. Zimmerman, S.P. Oncley, and A.C. Delaney, 1993: Atmosphere-surface exchange measurements. *Science.* **260,** 1472-1481.

Davis, D.D., F. Eisele, G. Chen, J. Crawford, G. Huey, D. Tanner, D. Slusher, L.Mauldin, S. Oncley, D. Lenschow, S. Semmer, R. Shetter, B. Lefer, R. Arimoto, A. Hogan, P. Grube, M. Lazzara, A. Bandy, D. Thornton, H. Berresheim, H. Bingemer, M. Hutterli, J. McConnell, R. Bales, J. Dibb, M. Buhr, J. Park, P. McMurry, A. Swanson, S. Meinardi, and D. Blake, 2004: An overview of ISCAT 2000. *Atmos. Environ.* **38,** 5363-5373.

Hanson, K.J., 1961: Some aspects of the thermal energy exchange on the south polar snow field and Arctic ice pack. *Mon. Wea. Rev.* **May 1961**, 173-177,

Howell, J.F., and J. Sun, 1999: Surface-layer fluxes in stable conditions. *Boundary-Layer Meteorol.* **90,** 495-520.

Humi, M., 2002. The case for 2d turbulence in Antarctic data. *Societa Italiana di Fisica*. **26,** 159-176. Kaimal, J.C., 1972. Turbulence spectra, length scales, and structure parameters in the stable surface layer. *Bound.- Layer Meteor.* **4,** 289-309.

Kailas, S.V and R. Narasimha, 1988: The structure of turbulence in a neutrally stable atmospheric boundary layer. IISc Report 88 FM 6 Dept of Aerospace Engineering, *Indian Institute of Science, Bangalore.*

Kaimal, J. C. and Finnigan, J. J.: 1994, *Atmospheric Boundary Layer Flows: Their Structure and Measurement*, Oxford University Press, Oxford, U.K.

Katul, G.G., J. Albertson, M. Parlange, C.-R. Chu, and H. Stricker, 1994: Conditional sampling, bursting, and the intermittent structure of sensible heat flux. *J. Geophys. Res.* **99,** 22869-22876.

Kelley, N.D., B.J. Jonkman, and G.N. Scott, 2005: The impact of coherent turbulence on wind turbine aeroelastic response and its simulation. *Windpower, 2005.*

King, J.C., and P.S. Anderson, 1994: Heat and water vapour fluxes and scalar roughness lengths over an Antarctic ice sheet. *Bound.-Layer Meteorol.* **69,** 101-121.

Kline, S.J., W.C. Reynolds, W.C. Schraub, and P.W. Runstadler, 1967: The structure of turbulent boundary layers. *J. Fluid Mech.* **30,** 741-773.

Kolmogorov, A. N., 1941.The local structure of turbulence in incompressible viscous fluid for very large Reynolds numbers. *Dokl. Akad. Nauk SSSR* **30**, 301- 305.

Mahrt, L., 1988: Intermittency of atmospheric turbulence. *J. of Atmo. Sci.* **46,** 79-94.

Mahrt, L. and D. Vickers, 1996: Quality control and flux sampling problems for tower and aircraft data. *J. of Atmo. And Ocn. Tech.* **14**, 512-526.

Nakamura, R. and L. Mahrt, 2005: A study of intermittent turbulence with CASES-99 tower measurements. *Bound.-Layer Meteorol*. **114**, 367- 387.

Nappo, C., 1991: Sporadic breakdowns if stability in the PBL over simple and complex terrain. *Bound.-Layer Meteorol.* **54.** 69-87.

Nappo, C., J. Cuzart, W. Blumen, X. Lee, and X-Z Hu, 2002: Intermittent turbulence associated with a density current passage in the stable boundary layer. *Bound.-Layer Meteorol.* **105,** 199-219.

Narasimha, R. and S.V. Kailas, 1987: Energy events in the atmospheric boundary later. *Perspectives in Turbulence Studies*. Springer-Verlag, Berlin. 188-222.

Narasimha, R. and S.V. Kailas, 1989: Turbulent bursts in the atmosphere. *Atmos. Environ.* **24A,** 1635-1645.

Oncley, S.P, M. Buhr, D.H. Lenschow, D. Davis, and S.R. Semmer, 2004: Observations of summertime NO fluxes and boundary-layer height at the South Pole during ISCAT 2000 using scalar similarity. *Atmos. Environ.* **38,** 5389-5398.

Salmond, J.A., and I.G. McKendry, 2005: A review of turbulence in the very stable nocturnal boundary layer and its implications for air quality. *Prog. In Phys. Geog.* **29**, 171-188.

Sodemann, H., 2002: Evaluation of a parameterization for turbulent fluxes of momentum and heat in stable stratified surface layers. Masters Thesis,*University of Bayreuth.*

Sorbjan, Z., 1985. Local similarity of spectral and cospectral characteristics in the stable-continuous boundary layer. *Boundary Layer Meteorology.* **35,** 257-275.

Stull, R.B., An Introduction to Boundary-Layer Meteorology. The Netherlands: Kluwer Academic Publishers, 1988.

Sun, J., S.P. Burns, D.H. Lenschow, R. Banta, R. Newsom, R. Coulter, S. Frasier, T. Ince, C. Nappo, J. Cuxart, W. Blumen, X. Lee and X. Hu, 2002: Intermittent turbulence associated with a density current passage in the stable boundary layer. *Bound.-Layer Meteorol.* **105,** 199-219.

Turner, J. and S. Pendlebury: *Antarctic Weather Forecasting Handbook.* British Antarctic Survey, 2004.

UCAR/NCAR: The Antarctic Mesoscale Prediction System (AMPS): 2007. http://www.mmm.ucar.edu/rt/wrf/amps/

Van De Wiel, B.: 2002, 'Intermittent Turbulence and Oscillations in the Stable Boundary Layer over Land', PhD Thesis, *Wageningen University, Netherlands.*

VanDop, H.: 2007, Boundary-Layer Meteorology, 94pp. **Preprint.**

Zilitinkevich, S.S., 2002: Third-order transport due to internal waves and non-local turbulence in the stably stratified surface layer. *Quart. J. Roy. Meteorol. Soc.,* **128,** 913-925.

APPENDIX A

FAST FOURIER TRANSFORMS AND THE CONVERSION FROM WAVE NUMBER TO FREQUENCY

(Methodology adapted from Stull, 1988)

Given the sinusoidal nature of atmospheric turbulence, Fourier analysis can be employed in order to convert the characteristics of a data set from being emphasized by wavenumber to being emphasized as a function of the frequency. And, as described by Stull (1988), the rules of Fourier transforms dictate that only a finite number of sine and cosine terms are required to fit the data set exactly. For spectral analysis, a forward Fourier transform is used, which allows for the conversion from physical space to frequencies.

An example in Stull (1988) dictates that when performing the Fourier transform, each data point in a set has a real part equal to the given value of the point, and an imaginary part of zero. Using Euler's formula, the data can be translated into functions of sines and cosines, as shown by equation A1.1, where *n* denotes the frequency, *k* the index of the data point, *N* the total number of points, and *A(k)* a representation of the original data set.

$$F_A(n) = \frac{1}{N}\sum_{k=0}^{N-1} A(k)\cos\left(\frac{2\pi nk}{N}\right) - \frac{i}{N}\sum_{k=0}^{N-1} A(k)\sin\left(\frac{2\pi nk}{N}\right) \quad \text{(A1.1)}$$

As an example for n=0, or the first data point, basic trigonometry dictates that all the cosines of zero are equal to one, and the sines are equal to one, giving A1.2,

$$F_A(0) = \frac{1}{N}\sum_{k=0}^{N-1} A(k) \tag{A1.2}$$

which can be interpreted as simply stating that the first point is represented by the algebraic mean of the data set.

Applying equation A1.1 over all data points then results in a set of data dictated by frequency, in which each frequency is represented by a real part of the original data, and an imaginary part of zero, as was previously stated. However, upon reaching the Nyquist Frequency, or, the frequency which is equal to one-half of the sampling frequency, all data points thereafter are complex conjugates of those prior to reaching the frequency. This allows for the use of fewer points in calculating the discrete energy spectrum, which is needed to discern the spectral characteristics of the dataset.

PERMISSION TO COPY

In presenting this thesis in partial fulfillment of the requirements for a master's degree at Texas Tech University or Texas Tech University Health Sciences Center, I agree that the Library and my major department shall make it freely available for research purposes. Permission to copy this thesis for scholarly purposes may be granted by the Director of the Library or my major professor. It is understood that any copying or publication of this thesis for financial gain shall not be allowed without my further written permission and that any user may be liable for copyright infringement.

Agree (Permission is granted.)

_____Julie Ann Phillipson_____ __05-02-2008_____
Student Signature Date

Disagree (Permission is not granted.)

_____ _____
Student Signature Date